

Nearshore hydrodynamics as loading and forcing factors for *Escherichia coli* contamination at an embayed beach

Zhongfu Ge,^{a,*} Richard L. Whitman,^a Meredith B. Nevers,^a Mantha S. Phanikumar,^b and Muruleedhara N. Byappanahalli^a

^aU.S. Geological Survey, Great Lakes Science Center, Lake Michigan Ecological Research Station, Porter, Indiana

^bDepartment of Civil and Environmental Engineering, Michigan State University, East Lansing, Michigan

Abstract

Numerical simulations of the transport and fate of *Escherichia coli* were conducted at Chicago's 63rd Street Beach, an embayed beach that had the highest mean *E. coli* concentration among 23 similar Lake Michigan beaches during summer months of 2000–2005, in order to find the cause for the high bacterial contamination. The numerical model was based on the transport of *E. coli* by current circulation patterns in the embayment driven by longshore main currents and the loss of *E. coli* in the water column, taking settling as well as bacterial dark- and solar-related decay into account. Two *E. coli* loading scenarios were considered: one from the open boundary north of the embayment and the other from the shallow water near the beachfront. Simulations showed that the embayed beach behaves as a sink for *E. coli* in that it generally receives *E. coli* more efficiently than it releases them. This is a result of the significantly different hydrodynamic forcing factors between the inside of the embayment and the main coastal flow outside. The settled *E. coli* inside the embayment can be a potential source of contamination during subsequent sediment resuspension events, suggesting that deposition–resuspension cycles of *E. coli* have resulted in excessive bacterial contamination of beach water. A further hypothetical case with a breakwater shortened to half its original length, which was anticipated to enhance the current circulation in the embayment, showed a reduction in *E. coli* concentrations of nearly 20%.

Beach water, as the interface between the land and coastal waters, is a dynamic physical and ecological system. The transport and fate of fecal indicator bacteria (FIB) in beach water not only have direct implications for human health in coastal areas (Nevers and Whitman 2005; Frick et al. 2008) but also constitute an integral influence on the coastal ecosystem. Recently, computational models allowing for a simulation of temporal and spatial variations of model variables have been developed to understand microbial water quality in open beach waters of Lake Michigan (Liu et al. 2006; Thupaki et al. 2010). Embayed (i.e., partially enclosed) beach waters have been of particular interest because of their significantly more complex hydrodynamic properties and the tendency to accumulate FIB and other contaminants (Grant and Sanders 2010).

The 63rd Street Beach of Chicago, a frequently closed beach, had by far the highest *Escherichia coli* concentration (geometric mean 140 MPN [most probable number], 100 mL⁻¹) among 23 recreational beaches along Chicago's 37-km Lake Michigan shoreline during 2000–2005. In comparison, the site with the second-highest *E. coli* concentration was Montrose Beach, with a geometric mean of only 77 MPN 100 mL⁻¹ (Whitman and Nevers 2008). Since typical meteorological (e.g., rainfall) and hydrodynamic (e.g., current and wave) events usually have spatial scales larger than 37 km, the unique situation of microbial contamination at 63rd Street Beach likely resulted from local factors. Unaware of any direct source of pollution in the vicinity of the beach, we suspected that the structure of

the embayment might have played a role. In fact, 63rd Street Beach has the longest breakwaters and the largest embayment surface area among all embayed beaches of the 23 sites. The 63rd Street Beach has two breakwaters of 133 m and 344 m long, while those of 31st Street Beach (geometric mean of *E. coli* concentration 62 MPN 100 mL⁻¹), for example, are 67 m and 108 m, respectively. A previous numerical study of 42 embayments in New England of the United States (Abdelrhman 2005) concluded that the flushing time of an embayment, defined as the time lapse for the mean concentration of a conservative tracer in the embayment to drop to 1/e (approximately 37%) of the initial value, can be best estimated by the length of the shoreline (bounded by two breakwaters) and the surface area, compared to other parameters, such as the volume, mouth–cross-sectional area, and average depth, of the embayment. For embayments with similar lengths of shoreline, longer breakwaters correspond to larger bounded surface areas and therefore longer times to flush. These findings are relevant to our study because, if the flushing of contaminants or FIB are slow, other effects, such as bacterial settling (deposition), might become comparable to the horizontal movements and hence complicate the transport process. However, since FIB are nonconservative because of their respective life cycles and biotic responses to environmental stresses (e.g., predation, sunlight inactivation, and loss of culturability), their transport processes likely deviate from the ideal flushing cases (Abdelrhman 2005).

In order to discover the cause of high microbial contamination at 63rd Street Beach of Chicago, a numerical current model based on the widely used

* Corresponding author: zge@usgs.gov

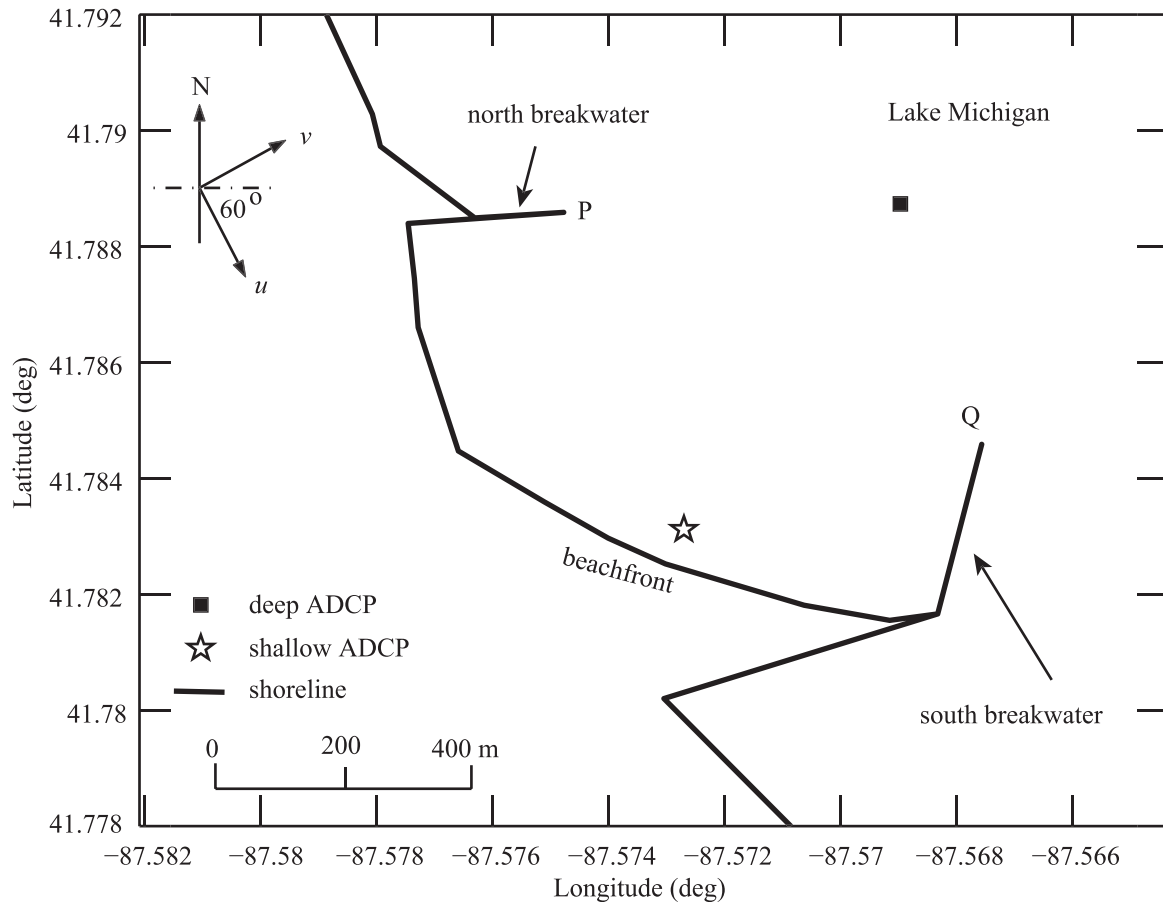


Fig. 1. Chicago's 63rd Street Beach. In this study, the u - and v -directions were defined to be 150° and 60° clockwise from the true north, respectively.

Princeton Ocean Model (POM) was developed. As an application of the numerical model in tracking the evolution of *E. coli* concentrations in the beach water, the bed sediment, and the decayed fraction, two important forcing and loading scenarios were considered. One scenario (referred to as case I in Results) reflects an *E. coli* receiving process of the embayment from an upcoast source forced by a main current coming out of the north. The other scenario (case II in Results) investigated the release of *E. coli* from shallow water in the embayment under a current circulation driven by a main stream out of the southwest. The difference between these two scenarios was expected to reveal the role of the embayment as a sink for FIB. More complex cases can be deduced as combinations of these fundamental scenarios. The numerical simulation, to be presented here, is also unique in modeling a hydrodynamic system that is significantly more complex than rivers or streams (Steets and Holden 2003; Bai and Lung 2005; Cho et al. 2010) and open coastal waters (Liu et al. 2006; Thupaki et al. 2010).

Since the embayment is a common design for numerous marine and freshwater beaches, the aim of the article was to explore the key processes that influence the fate and transport of FIB at embayed beaches. Our results were also expected to be significant in understanding the transport

of other ecologically important materials, such as algae, organic carbon, and nutrients, in coastal waters. Finally, the possibility of improving microbial water quality at the study site by shortening one of its long breakwaters was also explored (case III in Results).

Methods

Study beach—Chicago's 63rd Street Beach, a recreational beach in southwestern Lake Michigan, is shown in Fig. 1. The beach water is bounded by a shoreline and two breakwaters. The opening of the embayment is roughly toward the northeast. More detailed maps and area descriptions can be found elsewhere (Whitman and Nevers 2003; Olyphant and Whitman 2004).

For the purpose of collecting current data both inside and outside the embayment, two Acoustic Doppler Current Profilers (ADCP) were deployed at the locations indicated in Fig. 1 from late July through early August 2009. One ADCP was a Nortek 2-MHz Aquadopp current profiler (Nortek USA) at 41.7831°N and 87.5727°W , referred to as the shallow ADCP hereafter. It measured current velocity (averaged over 180 s) in four cells (cell size 0.3 m) at an interval of 12 min in approximately 1.4-m-deep water. Surface wave field was also measured every 24 min in a

burst mode that collected 1024 samples at a frequency of 2 Hz. Wave parameters, including significant wave height (H_s), peak period (T_p ; wave period corresponding to the peak component of the wave energy spectrum), and mean wave direction, were obtained by using Nortek's post-processing software. The other ADCP was a 600-kHz Workhorse Monitor (Teledyne RD Instruments; referred to as the deep ADCP hereafter) deployed at a depth of 6 m outside the embayment (41.7887°N and 87.5690°W). It measured current velocity with a frequency of 2 Hz averaged every 180 s. Up to 12 vertical cells were used, each with a size of 0.5 m. The distribution of water depth around the study beach was estimated by depth soundings on the day of ADCP deployment.

Numerical current model—The POM was employed for current simulation in the beach water. The POM (Mellor 2004) is a generic hydrodynamic model that uses semi-implicit finite-difference schemes to discretize fundamental equations of mass, momentum, and heat balances for three-dimensional fields of current velocity, salinity, temperature, and surface elevation in response to various inputs, such as wind, tides, and Coriolis forces. The model contains a second-order turbulence closure submodel that provides eddy viscosity and diffusivity for vertical mixing. In addition to marine water bodies, the POM has been successfully applied to the entire Lake Michigan (Beletsky and Schwab 2001) as well as considerably smaller areas, such as coastal waters in southern Lake Michigan (Thupaki et al. 2010). In contrast to open coastal waters (Thupaki et al. 2010), the embayed 63rd Street Beach has interesting flow structures, such as flow separation, recirculation (gyres) due to the blockage effect of the breakwaters, and the formation of turbulent shear layer near the opening of the embayment (Ge et al. 2010).

The depth-averaged current flow simulations around 63rd Street Beach resulting from longshore currents have been described previously (Ge et al. 2010). Briefly, a rectangular computational domain was used with its longshore side along the u -direction, as shown in Fig. 1 (i.e., 60° from the east), and a cross-shore side aligned with the v -direction. The computational domain was divided into 150 (longshore) by 75 (cross-shore) square grids with a uniform grid size of 13.92 m. Therefore, the lengths of the longshore and cross-shore sides are approximately 2 km (2088 m) and 1 km (1044 m), respectively. The computational domain is surrounded by both land and open-water boundaries. For the two-dimensional depth-averaged current simulations in the present study, the time step was set to 0.02 s to satisfy the model stability conditions (Mellor 2004) that became stringent for the embayed beach water. Model testing applied to this study is detailed in the Results section.

Decay rate of *E. coli* concentration—It has been well established that *E. coli* concentration in the water column is typically affected by environmental stresses, such as temperature, lack of nutrients, predation, and solar radiation. For modeling purposes in the present work, the decay rate for a particular set of *E. coli*, instead of that of *E. coli* in a particular water column (i.e., from the

Lagrangian point of view), was needed. A mesocosm study using 530-mL darkened (dark) and 200-mL transparent (light) WhirlPak bags that contained freshly collected water from Lake Michigan was conducted on a typical sunny day in June 2008. Hourly solar irradiance during the study period (24–25 June 2008) was observed from a HOBO weather station (Onset) placed at the study site (Fig. 2A). The difference between the dark and light bags was the permissibility of light penetration, so that *E. coli* in the dark bags underwent only dark loss of culturability, which is a resultant effect of natural death and predation, while those in the light bags decayed because of both dark base mortality and solar inactivation. Replicate dark and light bags with lake water were first suspended at middepth (20 cm below the water surface) in 45-cm-deep water at the beach at 04:00 h and then were exposed to the diurnal changes of temperature, solar irradiance, and wave motions throughout the day. Every hour from 08:00 h to 23:00 h, one dark and one light bag were randomly retrieved from the water. From 23:00 h to 07:00 h of the second day, bags were retrieved every 2 h. All samples were placed in coolers on ice, held at 4°C, and analyzed using the Colilert-18 method (American Public Health Association 1998) 4 h after collection. The light bags collected after 01:00 h of the second day were subject to excessive errors, and the associated data were not included in the analyses.

Over this diel period, *E. coli* concentration in the dark bags underwent a well-defined exponential decay, as shown in Fig. 2B, with a dark die-off rate k being approximately 0.0324 h^{-1} . The dark decay process of *E. coli* can therefore be expressed as

$$dc/dt = -kc \quad (1)$$

where c denotes *E. coli* concentration. The dark decay process was stable, insensitive to the diel variations of temperature. In the light bags, the effect of solar inactivation added to that of the base mortality and yielded a resultant decay process that cannot be described by a simple model similar to Eq. 1. It was found that the expression

$$dc/dt = -kc - k_I I c \quad (2)$$

best fit the results ($R^2 = 0.84$), where k is the same dark die-off rate as found in the dark bags (Eq. 1), I is solar irradiance as shown in Fig. 2A, and k_I , for this particular case, is approximately $1.254 \cdot 10^{-4} \text{ m}^2 \text{ W}^{-1} \text{ h}^{-1}$. Since *E. coli* regrowth in a natural freshwater environment is generally not significant in Lake Michigan, especially over a short period of time (e.g., 20 h), as focused in the present work, we used Eq. 2 for describing *E. coli* mortality rather than comprehensive, generic models proposed by Hipsey et al. (2008).

The recovery of solar-inactivated *E. coli* through deoxyribonucleic acid repair mechanism after the stress is removed is a complex process with both biotic and abiotic components. Previous laboratory studies have demonstrated a logarithmic dark repair rate of 20% (or a 0.01% rate in the original count) for *E. coli* at a nearly constant temperature of $23^\circ\text{C} \pm 1^\circ\text{C}$ after ultraviolet (UV)

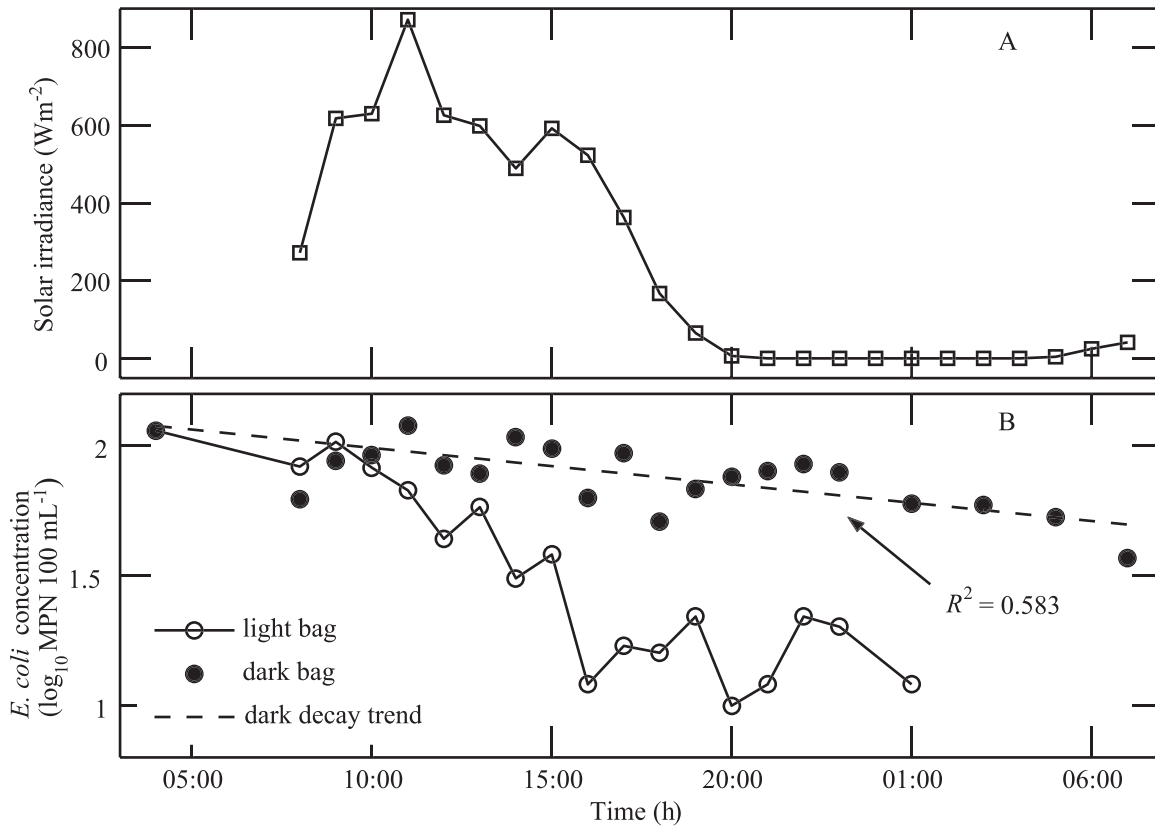


Fig. 2. An in situ mesocosm study conducted in June 2008 to estimate *E. coli* inactivation due to dark mortality and solar effects. (A) Solar irradiance observations on 24–25 June 2008; (B) hourly *E. coli* concentration in the light and dark bags revealing different decay processes.

disinfection (Hu et al. 2005; Quek and Hu 2008). Their dark repair case is comparable to the conditions of the present study, where *E. coli* would settle out of the sunlight-penetrated layer of water and eventually into the sediment. In what follows, therefore, no *E. coli* recovery was considered once they were inactivated by solar radiation, so that those *E. coli* cells were permanently removed from the system.

Transport-decay model for E. coli—A depth-averaged, advection–diffusion type of model coupled with a bacterial decay component was developed based on the SEDGL2D program of the National Oceanic and Atmospheric Administration (Lee et al. 2007). With a given current field obtained using, for example, the POM, the transport and decay of *E. coli* in coastal water is given as

$$\begin{aligned} \frac{\partial(hc)}{\partial t} + \frac{\partial(huc)}{\partial x} + \frac{\partial(hvc)}{\partial y} &= \frac{\partial}{\partial x} \left(D_{xx}h \frac{\partial c}{\partial x} + D_{xy}h \frac{\partial c}{\partial y} \right) \\ &+ \frac{\partial}{\partial y} \left(D_{yx}h \frac{\partial c}{\partial x} + D_{yy}h \frac{\partial c}{\partial y} \right) - w_s c \\ &- h(kc + k_I I c_0) \end{aligned} \quad (3)$$

where h denotes water depth; u , v are depth-averaged current velocity components in the x , y directions, respectively; c denotes the depth-averaged *E. coli* concentration; D_{xx} , D_{yy} , D_{xy} , and D_{yx} are the turbulent diffusion

and dispersion coefficients; and w_s denotes the nominal settling velocity of *E. coli* that is the product of the actual settling velocity of sediment (\bar{w}_s) and the fraction of sediment-attached *E. coli* (f_p). It is noted that the last term of Eq. 3 accounts for the dark and solar-related die-off based on Eqs. 1 and 2. This indicates that the transport-decay model (Eq. 3) describes only culturable *E. coli* concentrations. Inactivated *E. coli* that might still remain in the water column are not accounted for by the model. The transport model was implemented using the same grid used for the current simulations in POM. Alternating upwind (first-order) and Lax–Wendroff (second-order) schemes were used for discretizing Eq. 3. The time step was set to 0.1 h.

The settling velocity of sediment (\bar{w}_s) was set to 1.43 m d^{-1} or $1.65 \cdot 10^{-5} \text{ m s}^{-1}$ for the present study. This settling velocity was carefully selected on the basis of previous results in the literature, for example, Auer and Niehaus (1993) and Steets and Holden (2003), recognizing that *E. coli* colonies tend to attach to particles ranging from clay to fine silt. Although Stokes's law has often been used for determining the settling velocity (\bar{w}_s), it sometimes overestimates this value because of the flocculation of the fine particles that *E. coli* are most likely to attach to (Rehmann and Soupir 2009). Chapra (1997) tabulated measured settling velocities of particles found in natural waters. For clay (diameter 2–4 μm) and fine silt (diameter approximately 10 μm), the settling velocity is 0.3–1 m d^{-1} and 3 m d^{-1} , respectively. The value of 1.43 m d^{-1} used here is approximately the median of this observed range.

E. coli can be differentiated as either free swimming or particle bound. The fraction for sediment-attached *E. coli* (f_p) can vary considerably in different environments. Mahler et al. (2000) found that the attachment fraction of fecal coliform and enterococci to sediment particles in a creek and adjacent wells could range from 0.05 to 1.0 following rainfall events. On the other hand, in aquatic systems similar to the embayment studied here, previously measured attachment rates tended to be near 1.0. For example, Auer and Niehaus (1993) found that nearly all fecal coliform bacteria were associated with sediment particles in Lake Onondaga, New York, during the period of their experiment. Hipsey et al. (2006) estimated the attachment fraction of *E. coli* to be 0.94 in a freshwater reservoir in Australia. In our study, we simply set f_p to 1, and its uncertainty was absorbed into that of \tilde{w}_s , where now $w_s = \tilde{w}_s$. In the Results section, a range of w_s values centered around $1.65 \times 10^{-5} \text{ m s}^{-1}$ will be used to assess the sensitivity of simulations to the value of w_s .

For the transport model applied to the entire water volume, solar inactivation of *E. coli* tends to occur only in the surface layer that is within a certain depth from the water surface. This depth of light penetration at 63rd Street Beach can be estimated from previous observations based on the Beer–Lambert law. For instance, UV radiation was continuously measured 1 m above and 0.22 m below the water surface on 18 September (from 07:30 h to 15:00 h), which was a sunny day with calm lake conditions, and on 25 September 2000 (from 08:30 h to 14:30 h), a cloudy day with a strong east–northeast wind, moderately high waves, and turbid beach water (Whitman et al. 2004). Assuming an exponential decay of the UV radiation intensity, namely,

$$I(z) = I(0)e^{-\sigma z} \quad (4)$$

where I is the intensity of UV light, which is a function of water depth z , and σ denotes the extinction coefficient of light, we estimated that $\sigma = 3.370 \pm 0.488 \text{ m}^{-1}$ for 18 September and $\sigma = 12.238 \pm 1.254 \text{ m}^{-1}$ for 25 September. The extinction coefficient was fairly stable throughout the observation period on both days with a standard deviation of about 10% of their respective means. UV light appeared to attenuate much more rapidly with increasing water depth in turbid water than in clear water. Based on such extinction coefficients, we estimated the light penetration depth (z_s) to be 0.889 m for 18 September 2000 and 0.245 m for 25 September 2000, corresponding to a 5% residual intensity of light. It is noted that this penetration depth was only for the UV component of sunlight, but as UV radiation plays a critical role in the disinfection of bacteria, light penetration depths estimated based on UV data were believed to be representative. Therefore, *E. coli* concentration in the water column that is subject to solar-related inactivation (c_0) is only a fraction of c ; that is, $c_0 = (z_s/h)c$ (Eq. 3).

E. coli might also be resuspended into the water column. However, sediment resuspension is much more complex compared to settling, which was assumed to have an approximately constant vertical velocity in most previous works (Nielsen 1992; Chapra 1997). In the present study,

we considered only cases where no sediment resuspension occurred simultaneously with settling, such as a period after (but not during) a major resuspension event.

The diffusion coefficients of FIB, D_{xx} , D_{yy} , D_{xy} , and D_{yx} in Eq. 3 were often assumed to be negligible in similar studies. For example, Zhu et al. (2011) simulated the fate and transport of enterococci around a partially enclosed (bayside), low-energy, marine beach using a small grid size of 15 m near the shore, which was comparable to the present case with a grid size of 13.92 m. For such fine grids, physical diffusion tends to be negligible (de Brauwere et al. 2011) and can be simply compensated by numerical diffusion (Zhu et al. 2011). This is also the case for the present work. Hence, the diffusion coefficients in Eq. 3 were set to zero in the simulations. It was, however, noted that a future study for determining the diffusion characteristics in situ would be helpful for refining the numerical model used here.

Nondimensional form of the transport-decay model of E. coli—A dimensional analysis was further conducted for a better understanding of Eq. 3. For the water body *inside* the embayment, we selected the length of the south breakwater, B (344 m), as the horizontal length scale; a typical depth of the embayed beach water, H (e.g., 2 m), as the vertical length scale; a typical velocity magnitude U (e.g., 0.01 m s^{-1}) as the velocity scale; and a typical solar irradiance value I_0 (e.g., 400 W m^{-2}) in the day (Fig. 2A) as the scale for solar irradiance. The time scale can be derived as B/U . Denoting the nondimensional variables as primed symbols of their respective dimensional counterparts, we have

$$\frac{\partial(h'c')}{\partial t'} + \frac{\partial(h'u'c')}{\partial x'} + \frac{\partial(h'v'c')}{\partial y'} = -E_m c' - D_a h' c' - \tilde{D}_a h' I' z' c' \quad (5)$$

for Eq. 3, where $E_m = 2w_s/\beta U$ can be conveniently referred to as the *embayment settling number* because the ratio $\beta = 2H/B$ is approximately the slope of a linearly sloping beach and the ratio $w_s/\beta U$ reflects the settling velocity of *E. coli* in the beach water relative to the horizontal current velocity, $D_a = kB/U$ is the Damköhler number (Chapra 1997) for dark *E. coli* decay, $\tilde{D}_a = k_I I_0 B/U$ is the Damköhler number for solar inactivation of *E. coli*, and $z' = z_s/h$. Substituting the scale values into the right side of Eq. 5 yielded that $E_m \approx 0.28$, $D_a \approx 0.31$, and $\tilde{D}_a \approx 0.48$. This implies that settling, dark decay, and solar inactivation of *E. coli* in the embayment were all on the same scale as advection (left side of Eq. 5), and hence none of the factors was dominant.

For the water *outside* the embayment, on the other hand, the characteristic velocity magnitude U should be increased to that of the main current stream such as 0.15 m s^{-1} , which is 15 times larger than that inside the embayment. The scale of E_m was further reduced by the significant increase in the water depth H by approximately 2.5 times, that is, from 2 m for the embayed beach water to 5 m for the open water outside the embayment. No other characteristic parameters needed to be changed. These changes resulted in considerably diminished E_m (by 37.5 times), D_a (by 15 times), and \tilde{D}_a (by 15 times) outside the

embayment and hence the dominance of advection. Consequently, one of the most important characteristics of the coastal water modeled here was the clear division between the inside and the outside of the embayment in the characteristics of the transport and fate of bacteria.

E. coli mass accumulation—As *E. coli* settle to the lake bottom, the sediment receives *E. coli* mass. In the present study, we were interested only in the settled *E. coli* that had not decayed. Since in Eq. 3 the rates of change of *E. coli* due to settling and due to mortality occur simultaneously and are hence not differentiable, we must further hypothesize that the ratio of settled dead (nonculturable) *E. coli* to the total number of *E. coli* settled over a small (but finite) time step Δt was the same as that of the decayed *E. coli* (dark and solar related) to the total number of *E. coli* in the water column. Specifically, if culturable *E. coli* concentration in the sediment (settled out of the water column) (c_s) was defined to be directly comparable to that in the water, we obtained, in a discrete form,

$$\frac{\Delta c_s}{\Delta t} = \left[1 - \frac{(kc + k_I I c_0) \Delta t}{c} \right] \frac{w_s c}{h} \quad (6)$$

Apparently, when Δt approaches zero, the rate of accumulation of *E. coli* in the sediment is simply $w_s c/h$. This is consistent with Eq. 3, in which settling and decay are independent sink terms over an infinitesimal time step.

It has been well established that bottom sediment of various aquatic environments, marine or freshwater, is a reservoir for FIB (Goyal et al. 1977; Burton et al. 1987; Ishii et al. 2007). FIB, including *E. coli*, are able to survive in the sediment for a time period from 60 d to more than a year. Davies et al. (1995) found that throughout their 68-d experiment period, the same proportion of *E. coli* remained culturable, suggesting that sediment provided a favorable, nonstarvation environment for bacteria. Based on these observations, we assumed that there was no further decay for culturable *E. coli* in the sediment. This simplification should not result in significant error for the duration of simulation, which was 20 h, in the present work. Culturable *E. coli* stored in the bed sediment can be resuspended by natural causes or recreational activities and can be an important source of pollution (Goyal et al. 1977; Haller et al. 2009; Ge et al. 2010).

The concentration of decayed (i.e., nonculturable) *E. coli*, c_d , accumulates over time as

$$\frac{dc_d}{dt} = kc + k_I I c_0 \quad (7)$$

which is complementary to Eq. 3. By time marching, the increasing *E. coli* quantity in the bottom sediment that are still culturable and the *E. coli* quantity that has become nonculturable can be traced using Eqs. 6 and 7, respectively.

E. coli concentration observation in 2000—*E. coli* concentrations were monitored at 63rd Street Beach on 75 weekdays, generally from Tuesday to Thursday, from April to September 2000 (Whitman and Nevers 2003; Olyphant and Whitman 2004). Water samples were taken

at about 07:00 h each day in 45-cm (knee-deep) and 90-cm (waist-deep) waters at five transects, about 100 m apart from one another, along the beachfront. Samples were simultaneously collected from the offshore end of the south breakwater (near point Q in Fig. 1), where water was about 4 m deep. Samples were kept at 4°C and analyzed within 3 h for *E. coli* concentration by membrane filtration onto mTEC agar using method EPA/600/4-85 076 (Olyphant and Whitman 2004). The obtained data set was used here for the verification of the *E. coli* transport-decay model (Eq. 3).

Numerical wave model—The effect of surface waves is typically dominant compared to that of currents in generating bed shear stress, the driving force for sediment resuspension (Nielsen 1992). Knowledge of the distribution of wave parameters inside the embayment is helpful for estimating the potential pattern and intensity of sediment (*E. coli*) resuspension. For the study beach, the wave field in the embayment is generated by incident waves from deeper water of Lake Michigan. As waves enter shallower water, wave refraction occurs, during which wave rays adapt their directions of propagation according to the local water depth. At the same time, wave energy is dissipated gradually because of the bottom friction.

A simple numerical model developed by Lou and Massel (1994) as a modification on the mild-slope wave equation (Berkhoff et al. 1982) was used in the present work. Briefly, the model solves a set of governing equations,

$$\frac{\partial}{\partial x} (|\nabla s| \sin \theta) - \frac{\partial}{\partial y} (|\nabla s| \cos \theta) = 0 \quad (8)$$

and

$$\begin{aligned} \frac{\partial}{\partial x} (H_s^2 C C_g |\nabla s| \cos \theta) + \frac{\partial}{\partial y} (H_s^2 C C_g |\nabla s| \sin \theta) \\ = -\kappa \gamma H_s^2 C C_g \end{aligned} \quad (9)$$

for wave refraction and dissipation, respectively. In Eqs. 8 and 9, $s = \vec{\kappa} \cdot \vec{x} - \omega t$ is the phase function with $\vec{\kappa}$, \vec{x} , and ω being the wave-number vector, displacement vector, and wave frequency, respectively; ∇ is the horizontal gradient operator; θ denotes the wave direction with respect to the x -axis; H_s denotes significant wave height; C and C_g are wave phase and group velocities, respectively; $\kappa = |\vec{\kappa}|$; and γ is the wave damping factor. More details are given by Lou and Massel (1994), especially regarding the evaluation of γ . The model can also predict the location of wave breaking where the wave height reaches a certain proportion of the water depth. The proportion was empirically set to 0.8 (Dean and Dalrymple 1984) in the present work. For simplicity, the effect of wave diffraction was neglected since only cases with incident waves coming straight into the embayment (i.e., onshore waves) were considered in this study, so that the effect of diffraction, caused mostly by the obstruction of the breakwaters, would be minimal.

Bed shear stress and E. coli resuspension—Sediment resuspension occurs frequently at 63rd Street Beach, especially in relatively shallow water. During a resuspension

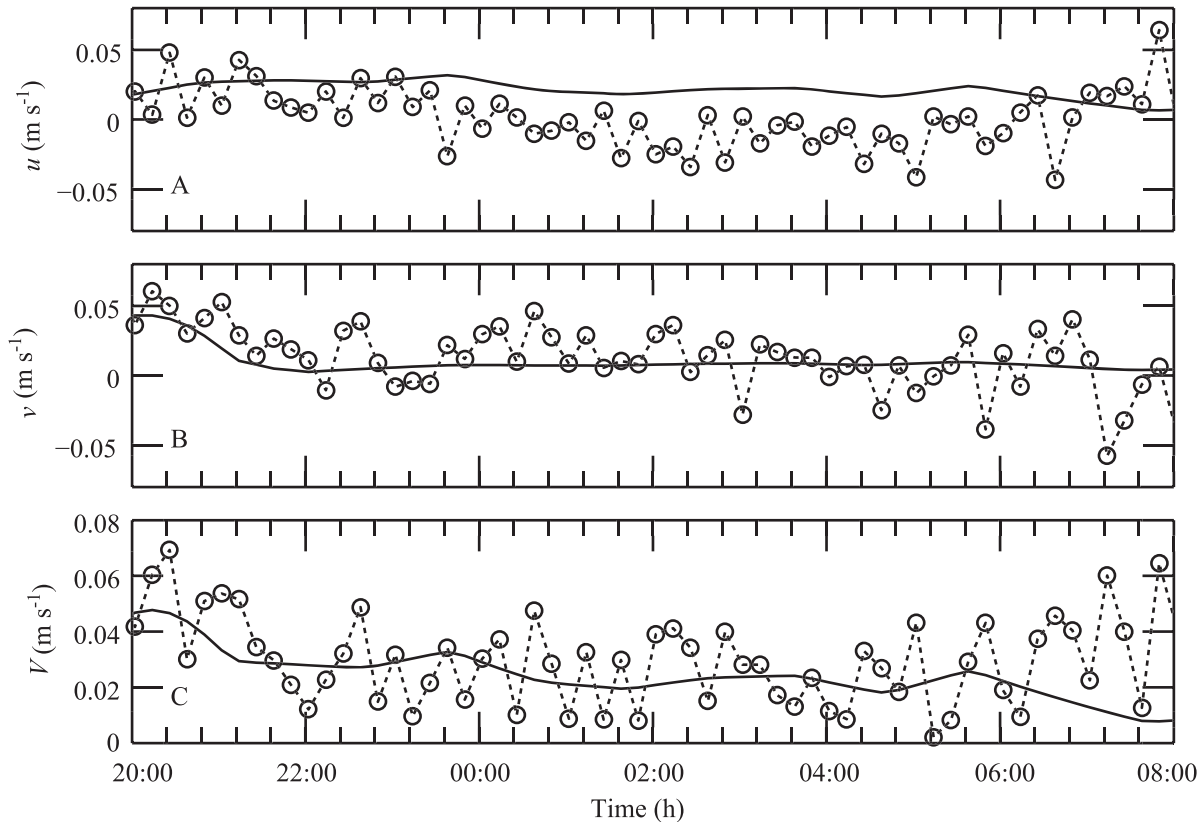


Fig. 3. Simulated (solid curve) and observed (circle) current velocity at the location of the shallow ADCP (see Fig. 1) during a 12-h period from 03 to 04 August 2009. (A) The u -component of the current velocity; (B) the v -component of the current velocity; (C) the magnitude $V = \sqrt{u^2 + v^2}$.

event, *E. coli*, most of which are sediment attached, are entrained back into the water column. A laser in situ scattering and transmissometry instrument (LISST-100X, Sequoia Scientific) was deployed on the lake bottom at the same location as the shallow ADCP (Fig. 1) during 05–18 August 2009 to analyze the particle size distribution of suspended sediment at a rate of 45 s per sample. The mean suspended particle size was found to be 0.0815 mm (see Results for details).

If both current and wave fields are known in the embayment, the bed shear stress τ can be estimated on the basis of a combined wave–current boundary layer following the method described by Grant and Madsen (1986) and applied to water quality modeling by Ge et al. (2010). Briefly, bed shear stress is determined by a nonlinear addition of wave and current boundary layers. The mean particle size measured in situ here was also a critical parameter in the evaluation of τ .

Low bed shear stress does not trigger sediment resuspension. The threshold value of τ for sediment suspension was often adopted between 0.05 and 0.1 N m^{-2} in Lake Michigan (Lou et al. 2000). In the present work, we used 0.06 N m^{-2} , below which no sediment was assumed to be resuspended. Since the simulation of a detailed sediment resuspension process was not attempted in the present work, the choice of the threshold value for resuspension, 0.06 N m^{-2} , was not a critical issue. The computed wave field and the resulting bed shear stress were used only to interpret the

spatial *E. coli* distributions as described later in the Results section.

Results

Numerical current model verification—Model testing was conducted for a period of 12 h from 03 to 04 August 2009. The embayment model was driven using the actual observations of current velocity (u and v) from the deep ADCP as a boundary condition. The downcoast boundary (south to the domain) was assumed to have a linearly decreasing v from offshore toward the land and a constant u equal to that at the offshore boundary. Since the current entered the domain mainly from the southeast during the simulation period, the upcoast boundary (north to the domain) therefore should represent an outlet for the current flow, assumed to have a uniform u -component determined by the mass balance of water entering and exiting the domain and a linearly decreasing v toward the shore. More details and justification for this choice can be found in Ge et al. (2010).

With boundary conditions described above, currents at the location of the shallow ADCP were simulated and compared to the currents actually observed (Fig. 3). The simulated results, reported every 10 min, appeared to have significantly less fluctuation than those observed. The root mean square errors (RMSE) between the simulated and observed u , v , and $V = \sqrt{u^2 + v^2}$ were 0.030, 0.020, and

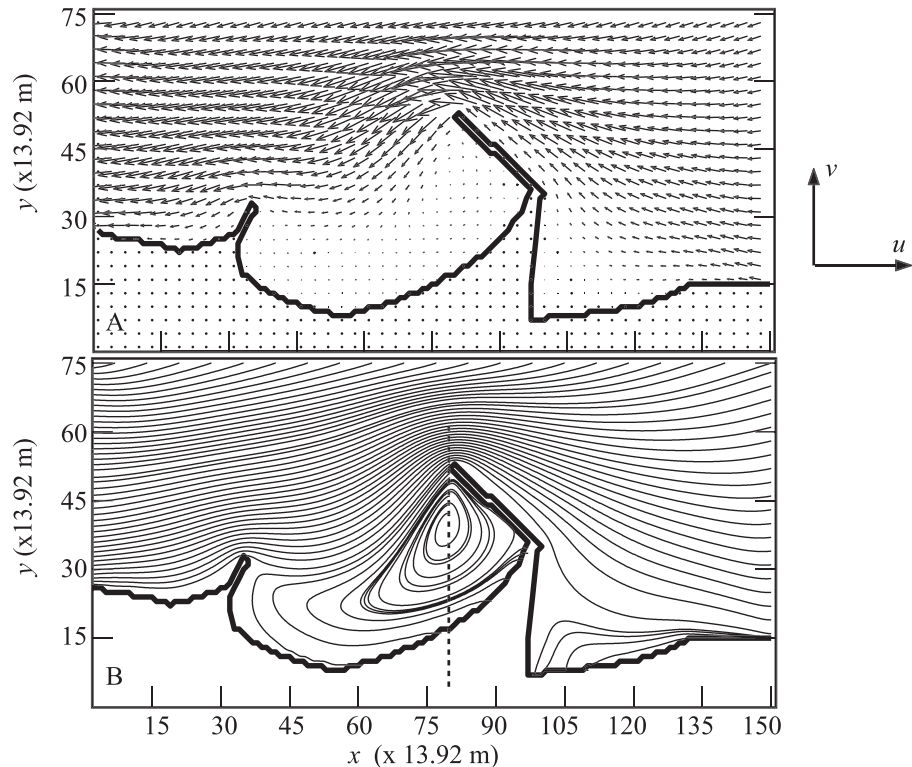


Fig. 4. Current pattern around the study beach driven by an upcoast longshore current entering the computational domain through the offshore (top) boundary with $u = -0.15 \text{ m s}^{-1}$ and $v = -0.05 \text{ m s}^{-1}$ and through the downcoast (right) boundary with $u = -0.15 \text{ m s}^{-1}$ and v decreasing linearly toward shore from -0.05 to 0 m s^{-1} and exiting at the upcoast (left) boundary with a uniform u and a linearly decreasing v from -0.05 to 0 m s^{-1} toward shore. (A) Current velocity vectors; (B) streamlines. For clarity, streamlines inside the embayment start at selected points along the dotted vertical line.

0.017 m s^{-1} , respectively. Since the magnitude of the current velocity was small, the error levels are acceptable. Potential sources of error included bathymetry, ADCP measurement errors, and the assumptions about the current velocity distribution at the open-water boundaries. However, since the focus of our work was on the key hydrodynamic processes operating at an embayed beach, we placed more emphasis on the trends and order of magnitude of the current fields as well as the general conclusions that we can draw from the analyses here.

A simulated current field—As an application of the numerical current model, a steady current field around the embayment of 63rd Street Beach was simulated. The simulation results will also be the basis of several cases in the remainder of the present work. The current field (Fig. 4) was driven by a longshore current entering the computational domain through the offshore ($u = -0.15 \text{ m s}^{-1}$, $v = -0.05 \text{ m s}^{-1}$) and downcoast ($u = -0.15 \text{ m s}^{-1}$, v decreasing linearly toward shore from -0.05 to 0 m s^{-1}) boundaries and exiting at the upcoast boundary with a uniform u and a linearly decreasing v from -0.05 to 0 m s^{-1} toward shore. The most conspicuous feature of the current pattern in the embayment was flow separation at the offshore end of the south breakwater and a large gyre generated by turbulent shearing. This gyre formed a local

recirculating pattern inside the embayment. Current velocity magnitude in the embayment appeared to be considerably smaller than that outside (Fig. 4A). The significant difference in the current pattern between the inside and the outside of the embayment supports the use of different sets of characteristic parameters in nondimensionalizing the model equation (Eq. 3) for these two sections of the flow system.

Numerical wave model verification—The numerically simulated wave parameters were compared with the actual observed data from the shallow ADCP during a 26-h period from 17:00 h on 22 July 2009 to 18:00 h of the next day. Hourly incident wave parameters were obtained from the Great Lakes Observing System (GLOS; www.glos.us) for Lake Michigan at the nearest grid point, approximately 1 km from the beach. Incident wave direction in deep water during this period was roughly onshore. The agreement between the simulated and observed significant wave heights, shown in Fig. 5A, was good with a correlation coefficient of 0.828 and an RMSE of 0.035 m. It is also noted that wave height at the location of the shallow ADCP was slightly larger than that of the incident waves, perhaps a prelude to wave breaking closer to the shore. An excellent agreement between simulated and observed wave directions is shown

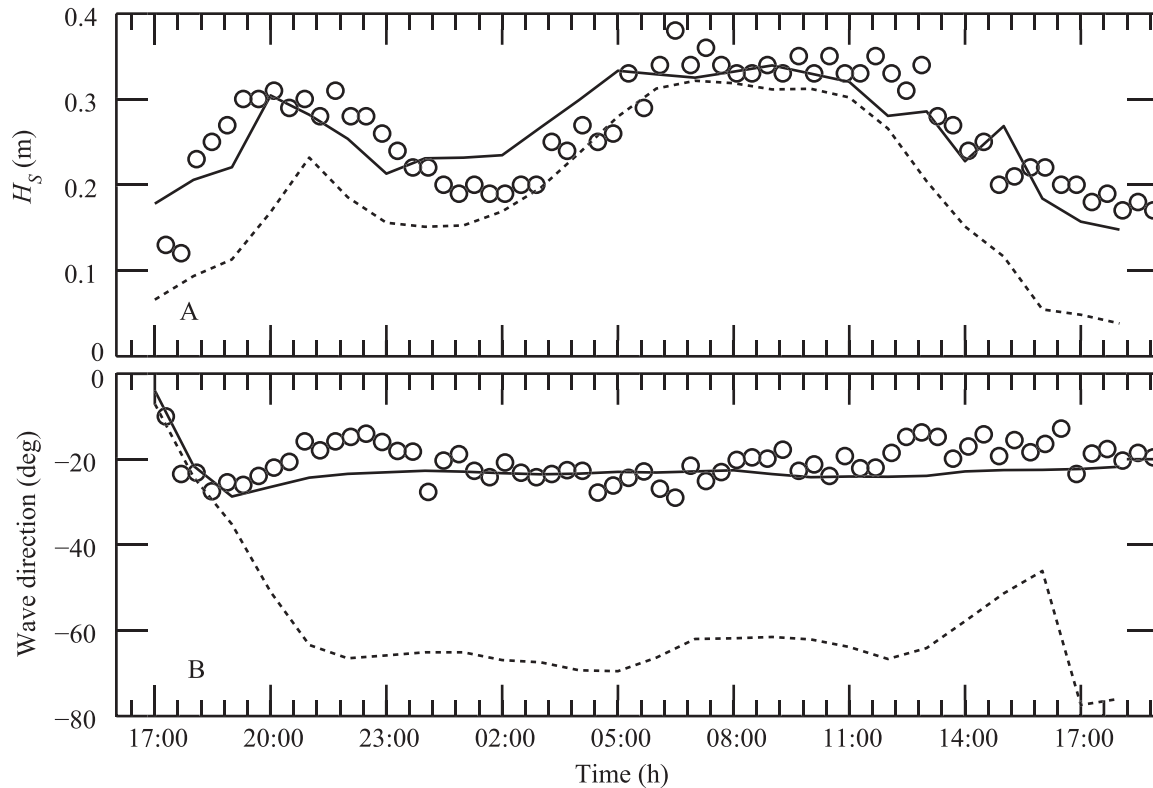


Fig. 5. Simulated (solid curve) and observed (circle) wave parameters in the beach water compared to the incident wave parameters (dotted curve) outside the embayment during a 26-h period from 17:00 h on 22 July 2009 to 18:00 h on 23 July 2009. (A) Wave height; (B) wave direction.

in Fig. 5B. The RMSE for the wave direction simulation was only 4.5° , and the largest difference between the simulations and the observations in the entire period was no larger than 10° . It is also interesting to see that the incident waves with a relatively wide range of directions, from -40° to -80° , were all refracted to have a direction of approximately -22° near the shore. The model performance compared favorably to that of previous applications of the similar model to, for example, wave propagation over an idealized shoal on a mild slope, which yielded more than 200% error between observed and simulated wave heights at multiple points over the shoal (Lou et al. 1996).

E. coli transport model verification—A comprehensive testing of the numerical *E. coli* transport-decay model is very difficult because the embayment at 63rd Street Beach can be affected by multiple bacteria sources. Model application requires initial and boundary conditions that include a precise spatial-temporal distribution of *E. coli* concentration for each source, demanding formidable survey and sampling efforts. In the present work, we tested the numerical model with observations from the year 2000.

Current velocity and wave parameters during the same period as the sampling project in 2000 (see Methods) were obtained from the GLOS at the nearest grid point described previously. In order to minimize the possibility of sediment

resuspension in the nearshore water as a bacteria source of unknown strength, we first selected cases with a significant incident wave height less than 0.25 m, which, we judged from previous experience, would be likely to resuspend bottom sediment only in the beach water shallower than 1.8 m. Cases (16 in total) with negative current velocity components u and v were further selected so that the main currents were approximately upcoast, representing upcoast flushing of the embayment. Without knowledge of the detailed distribution of current vectors along the open-water boundaries of the computational domain, we assumed a steady current field driven by a longshore current approaching the embayment from the southeast, which is the case shown in Fig. 4.

Since the minimum water depth considered here was 1.2 m, observed *E. coli* concentration in the 90-cm-deep water was a reasonable estimate for water up to 1.2 m deep. In water deeper than 1.2 m but shallower than 1.8 m, *E. coli* concentration was linearly extrapolated on the basis of those observed in the 45-cm- and 90-cm-deep waters. Since we assumed no additional *E. coli* sources, *E. coli* concentration was set to zero elsewhere. *E. coli* concentration in the water up to 1.8 m deep formed the boundary conditions for the simulation for each day. Within a few hours, the initial *E. coli* distribution in the shallow water in the embayment began to affect the deeper water as a traveling plume. The simulated *E. coli* concentrations were compared to the observed values at the offshore end of

Table 1. Comparison between observed and predicted *E. coli* concentrations (MPN 100 mL⁻¹) in 2000. The *E. coli* transport-decay model (Eq. 3) was used for prediction.

Date in 2000*	Observed <i>E. coli</i> concentration			Predicted <i>E. coli</i> concentration	
	0.45 m deep	0.9 m deep	4 m deep	4 m deep	Hours (h)†
18 April	41	42	7	4	11
20 April	240	200	10	11	7
18 May	2344	1995	83	93	6
01 June	94	95	20	8	10
06 June	37	30	3	2	11

* The 5 d all had significant wave height less than 0.25 m (presumably no *E. coli* resuspension in water deeper than 1.8 m); current velocity components $u < 0$, $v < 0$; and observed *E. coli* concentration in 0.9-m-deep water above 15 MPN 100 mL⁻¹.

† Lapse of time for *E. coli* concentration at point Q (Fig. 1) to attain the associated predicted level.

the south breakwater (point Q in Fig. 1). While *E. coli* concentration was originally reported in colony forming units (CFU) 100 mL⁻¹ in 2000, the same values in MPN 100 mL⁻¹ were used here to be consistent with the units in the numerical model (Eq. 3). *E. coli* concentrations estimated by these two methods—membrane filtration and the most probable number—have been found comparable in previous laboratory comparisons (Eckner 1998).

Of the 16 cases available, Table 1 shows 5 d on which the observed *E. coli* concentration in the 90-cm-deep water

was higher than 15 MPN 100 mL⁻¹. The numerical model appeared to predict the offshore *E. coli* concentration accurately, or at least with the correct order of magnitude. The time lapse for the offshore (4-m-deep) water to be affected by the shallow-water *E. coli* distribution was fairly short for all cases, which is not inconsistent with the simultaneity of the sample collections. The observed *E. coli* concentrations in the 90-cm-deep and the offshore waters for the remaining 11 cases were all very low (e.g., less than 15 MPN 100 mL⁻¹ in the 90-cm-deep water and less than

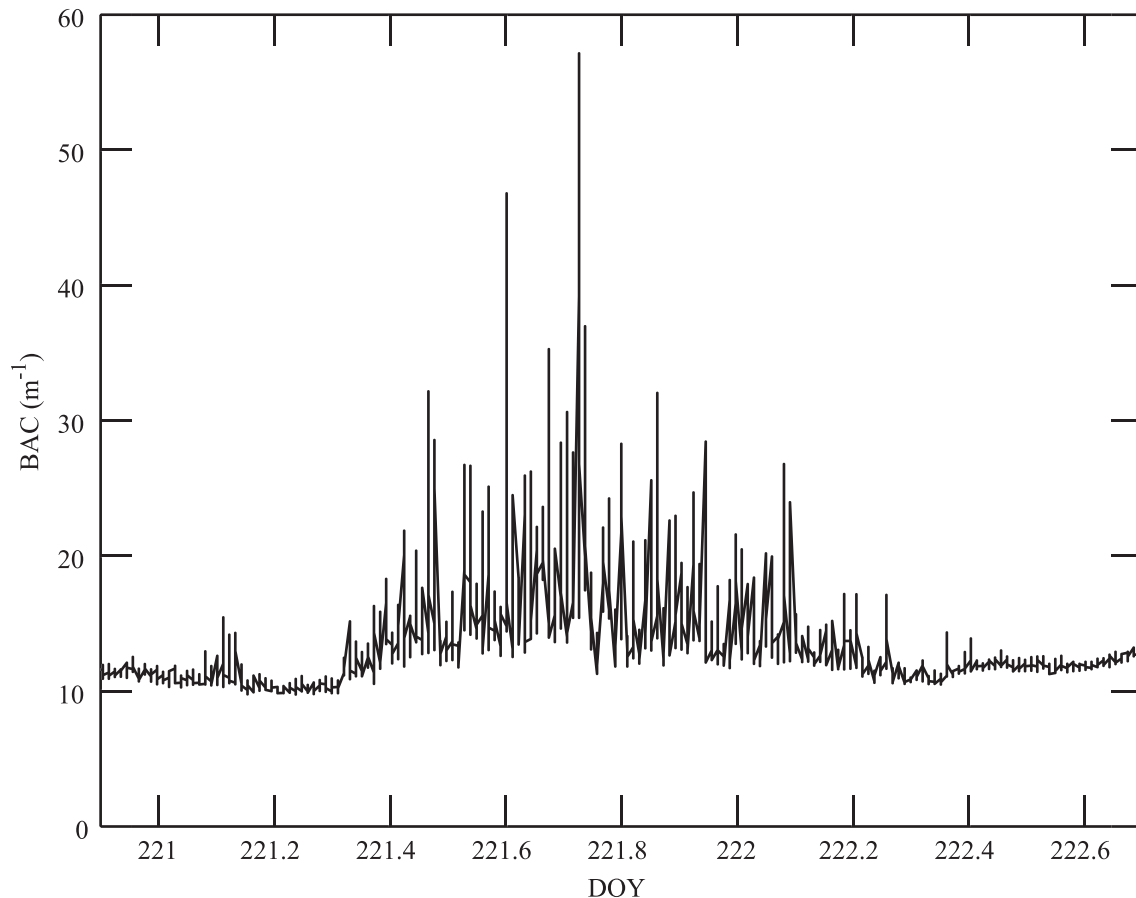


Fig. 6. Time series of the beam attenuation coefficient (BAC) measured with a LISST-100X instrument at the location of the shallow ADCP at 63rd Street Beach (Fig. 1) from days of the year (DOY) 220 (08 August) to 222 (10 August) of 2009. The bursts centered at DOY 221.7 signified a sediment resuspension event.

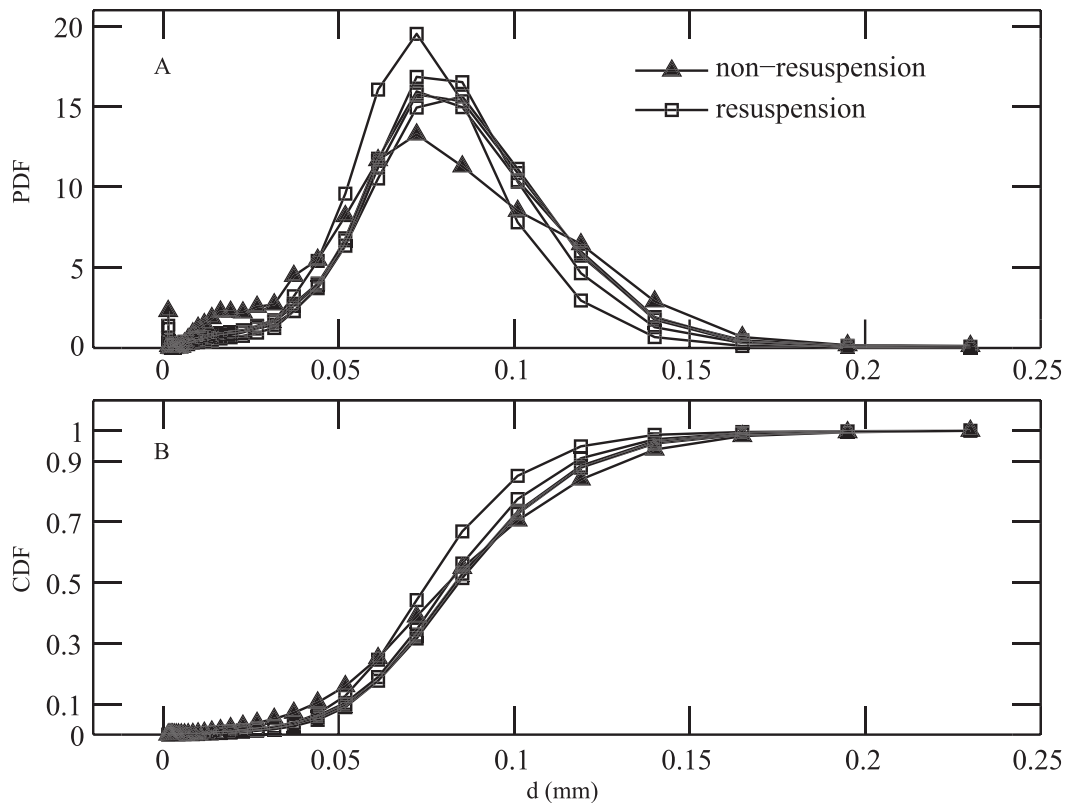


Fig. 7. Particle size distributions measured at 63rd Street Beach at DOY 221.2 (nonresuspension) and at five instants near DOY 221.7 (resuspension) of 2009. (A) Probability density function (PDF); (B) cumulative density function (CDF); the median sediment diameter was estimated to be 0.0815 mm.

5 MPN 100 mL⁻¹ in the 4-m-deep water). Predicted *E. coli* concentrations were consistently near zero in the offshore water for those 11 cases.

Characteristics of bed sediment and sediment resuspension—An episode of sediment resuspension was identified, for example, on 09 August 2009 from the beam attenuation coefficient (BAC) measured by the LISST (Fig. 6). The BAC value is well correlated with the concentration of suspended particulate material (Hawley and Lee 1999). The particle size distributions represented by the probability density functions (PDF) and the cumulative density functions (CDF) for one nonresuspension (at approximately day 221.2) and five resuspension (around day 221.7) cases during the period of time shown in Fig. 6 were arbitrarily selected and shown in Fig. 7. While the probability distributions of particle sizes for resuspension and nonresuspension cases were slightly different (Fig. 7A), the median diameter of sediment particles, corresponding to a CDF value of 0.5, was evidently insensitive to the occurrence of resuspension (Fig. 7B). The average of the median particle diameters for these six cases in Fig. 7 was 0.0815 mm, and thus this was used as the mean particle size in the sediment for further estimation of the bed shear stress. Compared to the mean bottom sediment size at four locations near the eastern shore of Lake Michigan (Muskegon, Michigan), which were in a range from 0.14 to 0.26 mm (Hawley and Lee 1999), the sediment at 63rd Street Beach was much finer.

To assess the pattern of sediment resuspension, we first simulated a wave field inside the embayment generated by incident random waves with $H_s = 0.35$ m, $T_p = 2.5$ s, and at an angle of -30° with the y -direction (Fig. 8). According to the data collected from the shallow ADCP from July to August 2009, 5% of the measured significant wave heights exceeded 0.35 m ($n = 1000$). The highest wave recorded there was 0.49 m.

Putting together this wave field and a current field such as the one shown in Fig. 4, we were able to estimate the bed shear stress that would result in sediment resuspension. Figure 8 shows the distribution of bed shear stress (τ) that exceeded 0.06 N m⁻² inside the embayment. Apparently, the distribution of bed shear stress above the threshold is fairly consistent with that of water depth, with most of the sediment resuspension occurring in the water shallower than 1.83 m.

Influence of bacteria loading from upcoast (case I)—As stated previously, the goal of our study was to assess the influence of typical current and bacteria loading patterns on the transport and fate of *E. coli* at an embayed beach. Realistic situations might not be as ideal as the cases evaluated here, but ideal, steady cases have the advantage of isolating key loading and forcing factors from all coincident events.

For case I, we assume that a longshore current traveled downcoast and formed a double-gyre circulation pattern in the embayment (Ge et al. 2010). This current pattern also

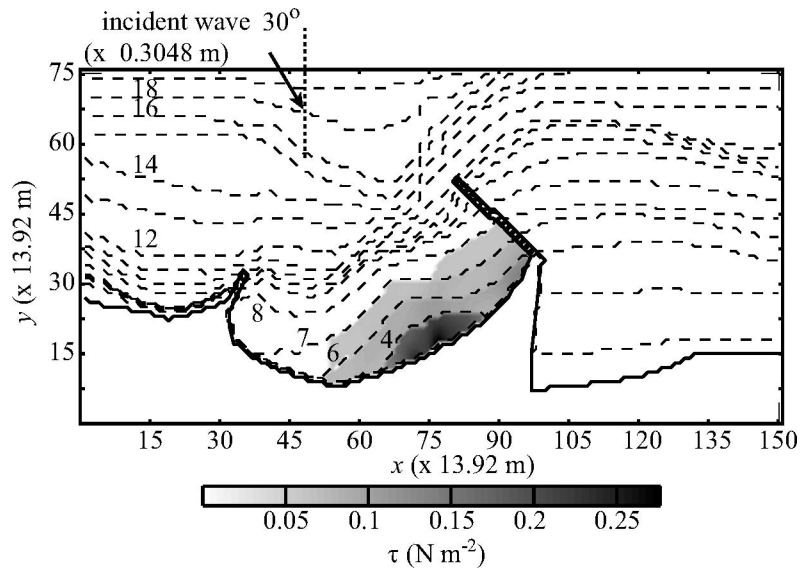


Fig. 8. Distribution of bed shear stress τ in the embayment resulting from an incident onshore wave field with $H_s = 0.35$ m, $T_p = 2.5$ s, and an angle of incidence of -30° . Solid curve: shoreline; dashed curve: contours of the bathymetry with water depths indicated. Bed shear stress τ was cut off at 0.06 N m $^{-2}$.

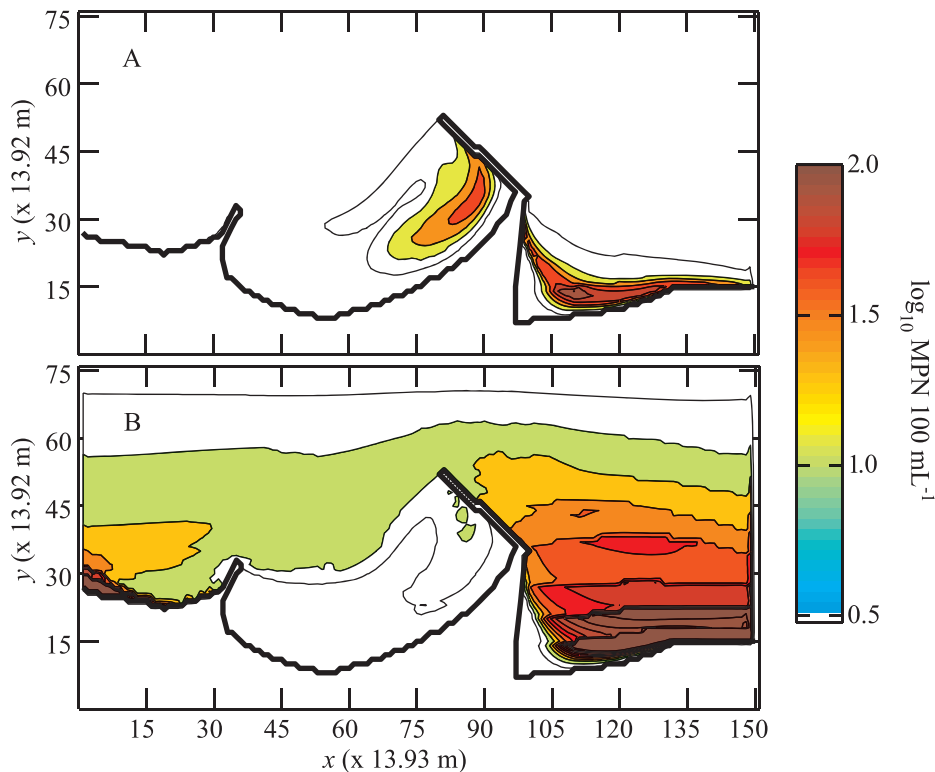


Fig. 9. Distributions of *E. coli* concentration at the 20th hour due to a loading from the north of the beach (case I). Current flow around the embayment was driven by a longshore current entering the computational domain through the upcoast boundary ($u = 0.15$ m s $^{-1}$, $v = 0$ m s $^{-1}$), exiting at the downcoast boundary (uniform u and zero v determined by mass balance in the computational domain), and with no flux at the offshore boundary. The current pattern can be found in Ge et al. (2010). *E. coli* loading was given at the upcoast boundary with concentrations decreasing from 150 MPN 100 mL $^{-1}$ at the shoreline to zero at the offshore end of the boundary during the first 10 h and zero afterward. (A) Suspended culturable *E. coli* concentration; (B) settled culturable *E. coli* concentration.

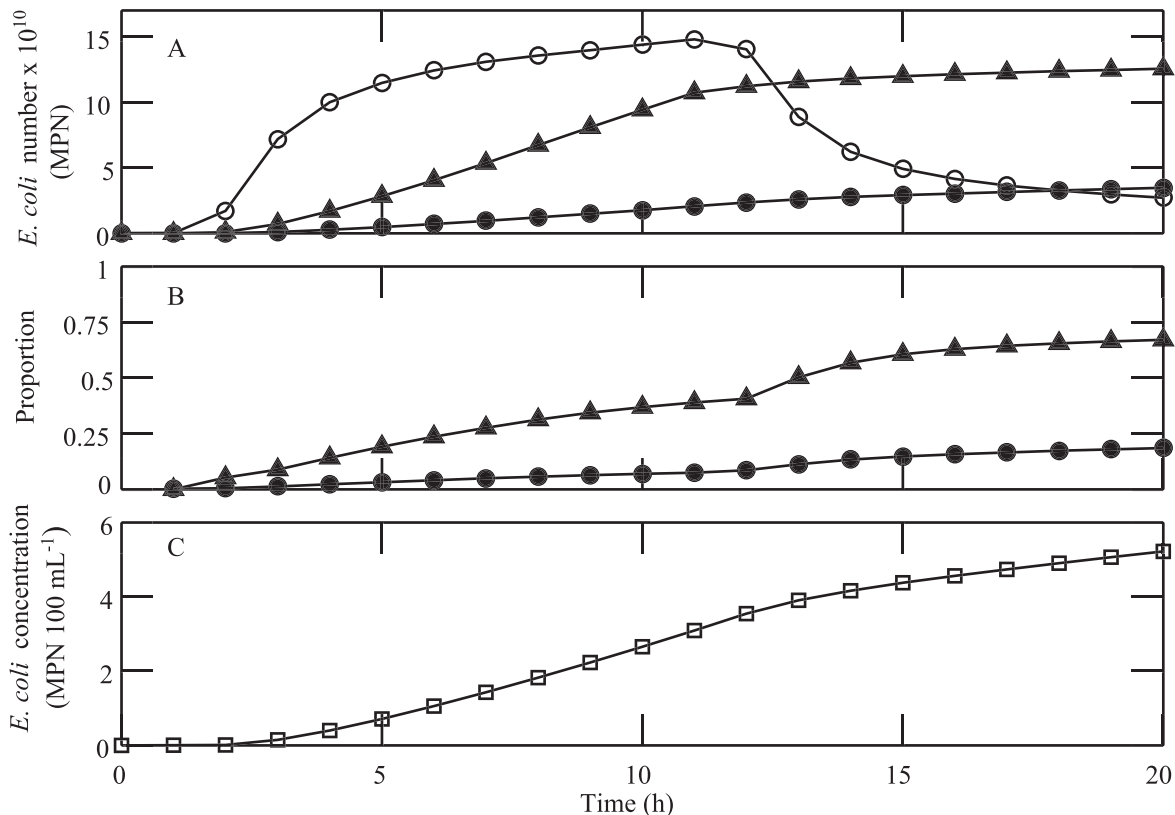


Fig. 10. *E. coli* budget in the embayment due to a longshore downcoast loading (case I). (A) Time history of the total suspended culturable (open circle), settled culturable (filled circle), and decayed (triangle) *E. coli* quantities (MPN) in the embayment; (B) the proportions of settled culturable (filled circle) and decayed (triangle) *E. coli* numbers within the total *E. coli* number in the embayment; (C) potential mean *E. coli* concentration in the embayed beach water when the settled culturable *E. coli* are all resuspended.

carried *E. coli* downcoast and into the embayment. A steady *E. coli* concentration was set at the upcoast boundary of the computational domain with a linear decrease from 150 MPN 100 mL⁻¹ at the shoreline to zero at the offshore end of this boundary. This loading was steady for the first 10 h, and afterward only clean lake water flowed by the embayment. In the first 10 h of this 20-h simulation, solar irradiance followed the actual variation pattern between 08:00 h and 19:00 h, as shown in Fig. 2A, and the light penetration depth was set to 0.889 m, as for a sunny and calm day. Solar irradiance was zero for the last 10 h. This ideal case was used to reveal how the embayment received *E. coli* from upstream sources, for example, 57th Street Beach, which was only about 400 m north (Whitman and Nevers 2008).

It is clear from Fig. 9A that after the *E. coli* loading and the washing of clean water, very little *E. coli* remained in the water outside the embayment, except for the zone shielded by the south breakwater. A plume of *E. coli*, however, was still approaching the shoreline inside the embayment and was only approximately 50 m from the beachfront. *E. coli* concentration at the center of this plume was up to 40 MPN 100 mL⁻¹. Given more intensive and persistent loading of *E. coli* from the north, the beach water quality would be more negatively influenced.

The accumulated deposition of culturable *E. coli* on the lake bed at the 20th hour was estimated (Fig. 9B). It is noted that a large quantity of culturable *E. coli* cells had

settled into the sediment both outside and inside the embayment.

A time history of the total numbers of *E. coli* inside the embayment (i.e., the water body bounded by the two breakwaters, the beachfront, and the line that connects points P and Q in Fig. 1) that were still culturable and suspended in the water, culturable but had settled in the sediment, and nonculturable are presented in Fig. 10A. Figure 10B shows the proportions of the settled, culturable and nonculturable *E. coli* numbers within the total number of *E. coli* that had so far entered the embayment. It can be deduced from Fig. 10A,B that the quantity of culturable *E. coli* in the embayed water culminated at the 11th hour, after which the effects of decay and settling became dominant. The effect of bacterial decay was significantly larger than that of settling throughout the simulation period, while about 20% of the total *E. coli* that had entered the embayment had been deposited into the sediment, remaining culturable, by the end of the simulation period. The results so far implied that a downcoast loading of contaminants by a longshore current field can appreciably affect the embayed beach within a day and deposit a fairly large amount of *E. coli* into the embayment. Furthermore, as an example, the hourly *E. coli* concentration resulting from uniformly distributing all the settled *E. coli* back into the embayed beach water is shown in Fig. 10C. This hypothetical *E. coli* concentration approached 6 MPN

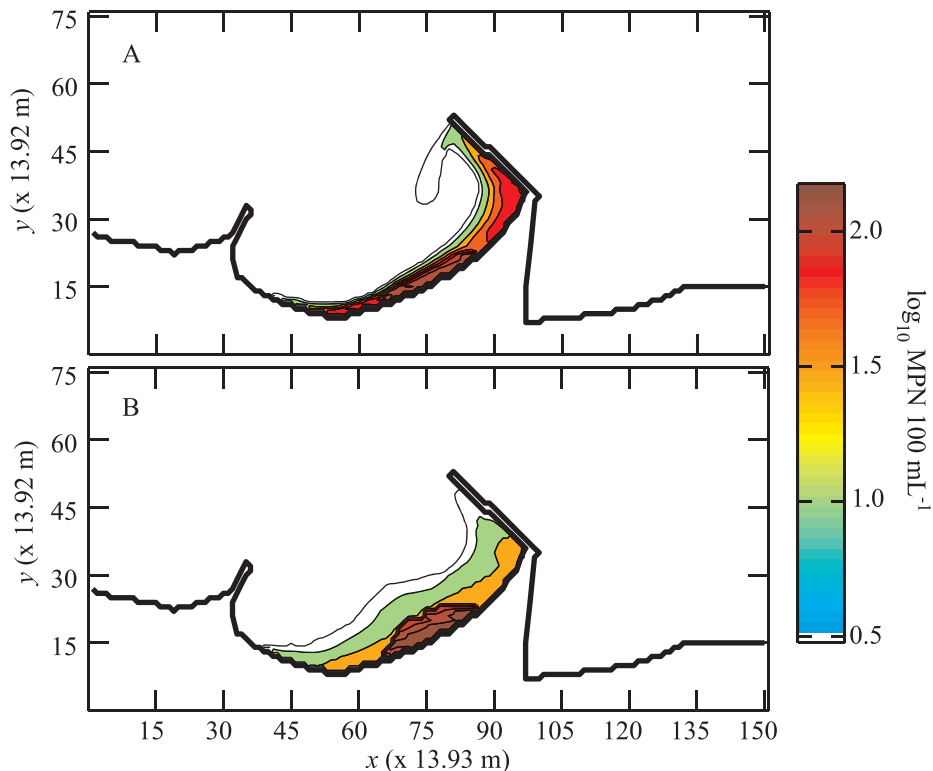


Fig. 11. Distributions of *E. coli* concentration at the eighth hour after a resuspension event in the embayment (case II). Initial *E. coli* concentration was given at 200 and 100 MPN 100 mL⁻¹ in waters less than 1.22 m deep and 1.83 m deep, respectively, in the embayment and zero elsewhere. (A) Suspended culturable *E. coli* concentration; (B) settled culturable *E. coli* concentration.

100 mL⁻¹ at the 20th hour, which roughly reflected the intensity of the potential *E. coli* source released during future resuspension events.

Releasing of resuspended E. coli (case II)—Here, we only assumed that the occurrence of sediment (bacteria) resuspension was highly correlated with the value of bed shear stress. As a simple case, after a relatively severe episode of wave actions (e.g., with incident $H_s = 0.35$ m, $T_p = 2.5$ s, and propagating precisely into the embayment) diminished, there was assumed to be a distribution of *E. coli* with a concentration of 200 and 100 MPN 100 mL⁻¹ in the waters up to 1.22 m and 1.83 m deep, respectively, in the embayment and zero elsewhere. This resuspended *E. coli* distribution pattern was consistent with that of the bed shear stress above the threshold shown in Fig. 8. No new *E. coli* source was imposed thereafter. The *E. coli* concentration field was transported and dispersed by the steady current field described in Fig. 4 for the next 20 h, affected by the same solar irradiance pattern as case I but with a light penetration length of 0.245 m as for turbid water. Figure 11A,B shows the distributions of culturable *E. coli* concentration that were still suspended in the water and that had settled back into the bottom sediment, respectively, at the eighth hour. It is notable that by the eighth hour (i.e., significantly less than a day), the resuspended *E. coli*

had already reached the opening of the embayment. This is consistent with the statistically inferred transport path of *E. coli*, which starts from the shoreline, passes the central area, and reaches the mouth of the embayment under such hydrodynamic conditions (Ge et al. 2010). It was also observed that the bottom sediment in the deeper water (up to 2.13 m) of the embayment had received and accumulated culturable *E. coli* (Fig. 11B). By the 20th hour (figure not shown), most initially suspended *E. coli* had either settled or decayed, except in the very shallow water (1.22 m deep). A larger area of the lake bottom in the embayment (i.e., up to about 3.05 m deep) had received *E. coli* deposition compared to the 1.83-m-deep water initially.

In contrast to the case with a downcoast *E. coli* loading (Figs. 9, 10), the transport of *E. coli* after a resuspension event was considerably diminished by settling and decay. Specifically, about 37.3% of the *E. coli* initially resuspended in the shallow water eventually settled back into the sediment inside the embayment, during which period nearly 54.1% of the total *E. coli* became nonculturable. Consequently, only 8.6% of the total *E. coli* could be eventually released live out of the embayment (Fig. 12). The deposited *E. coli* in the sediment would give rise to an average concentration of up to 10 MPN 100 mL⁻¹ if they were suspended again and redistributed uniformly in the entire embayment (Fig. 12C).

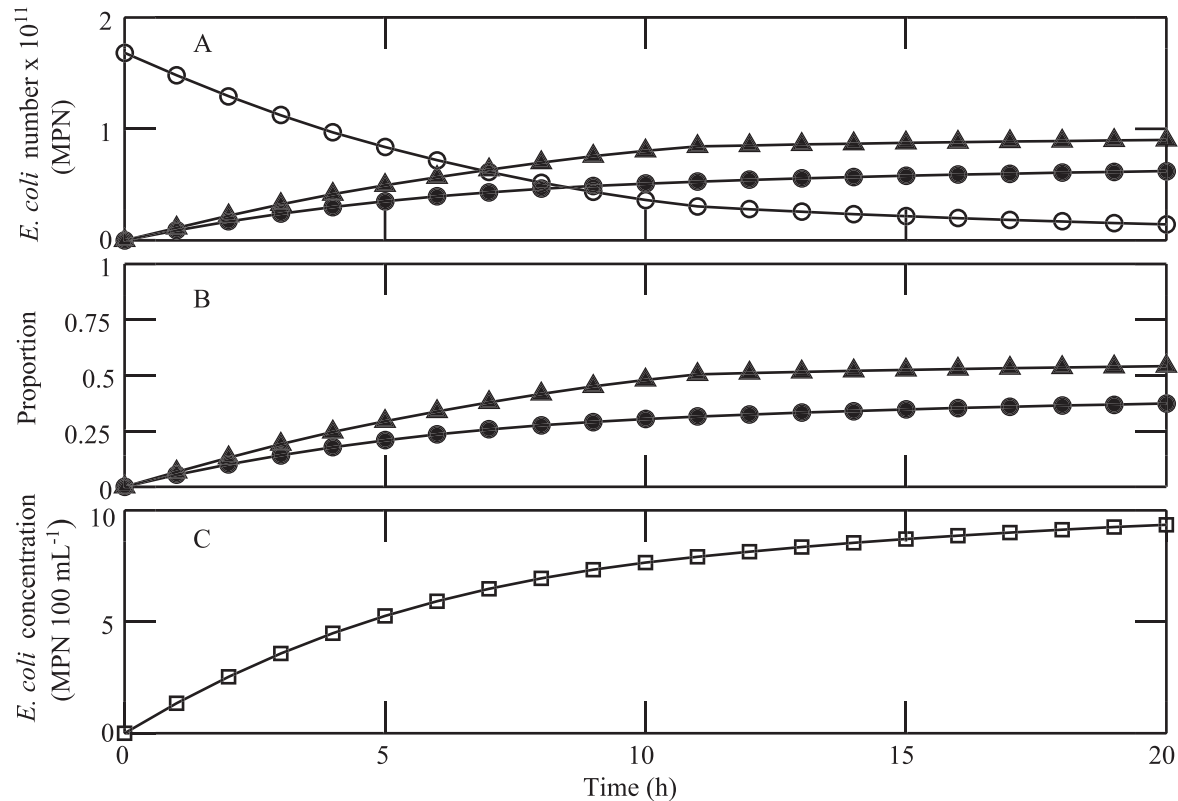


Fig. 12. Same as Fig. 10 but due to an initial *E. coli* distribution, as described in Fig. 11 (case II).

Releasing of resuspended E. coli with a hypothetically shortened breakwater (case III)—This case had the same setting as case II but with a hypothetically shortened south breakwater of 172 m, half the actual length. The resulting current field is shown in Fig. 13, which can be directly compared to Fig. 4 for an assessment of the influence of the south breakwater on the flow field. It seemed that the shortening of the breakwater from the offshore end would break the large single-gyre pattern inside the embayment, as for the original case, into two smaller gyres. The flushing of the embayment appeared to be enhanced to a certain extent because the main current stream could intrude deeper into the embayment compared to case II (Fig. 13B). Strong nonlinearity in this hydrodynamic system was also manifested by the change from a single- to a double-gyre current pattern on reducing the breakwater length in the sense that no similarity in the flow pattern was preserved by changing the geometry of the boundaries.

The *E. coli* concentration distribution in the water at the eighth hour (Fig. 14A) is similar to that for case II (Fig. 11A) near the south breakwater but there is also a tendency for part of the *E. coli* to concentrate around the other gyre near the north breakwater. Table 2 further summarizes the possible improvement of microbial water quality compared to case II in terms of the total culturable *E. coli* number in the embayed beach water and in the submerged sediment (as a potential source that can be released by future resuspension events) at the 10th and 20th hours, respectively. It is clear that a 50% reduction in the breakwater length from the offshore end would result in a

19% reduction in the *E. coli* count inside the embayment and an 11% reduction in the *E. coli* supply from the bed sediment for the future.

Simulation sensitivity to the value of the settling velocity—The value of the settling velocity might affect the simulation results to a certain extent. Two cases in the same setting as case II but with a settling velocity that is half (i.e., $0.82 \times 10^{-5} \text{ m s}^{-1}$) and double (i.e., $3.3 \times 10^{-5} \text{ m s}^{-1}$) the value used in case II ($1.65 \times 10^{-5} \text{ m s}^{-1}$), respectively, were examined. As shown in Table 3, the proportion of suspended culturable *E. coli* within the total *E. coli* number in the embayment responded approximately linearly to the variation of the settling velocity value. For instance, when the settling velocity was doubled (i.e., faster deposition), the associated proportion for suspended *E. coli* was reduced to approximately half the value for case II. The response of the proportion of settled culturable *E. coli* within the total *E. coli* also appeared to be linear. While the results are inadequate to draw any general conclusions, the two additional cases at least implied a possible range of model response to the uncertainty in the settling velocity value. Specifically, it was deduced that the proportion of suspended *E. coli* that could be released live out of the embayment would be possibly from 4.5% to 16.6% of the total *E. coli* number. The proportion of settled culturable *E. coli*, which could be a source of fecal contamination in the future, would be from 21.2% to 47.9%. The results are thus consistent with those from case II: a significant percentage of the initially resuspended *E. coli* would settle

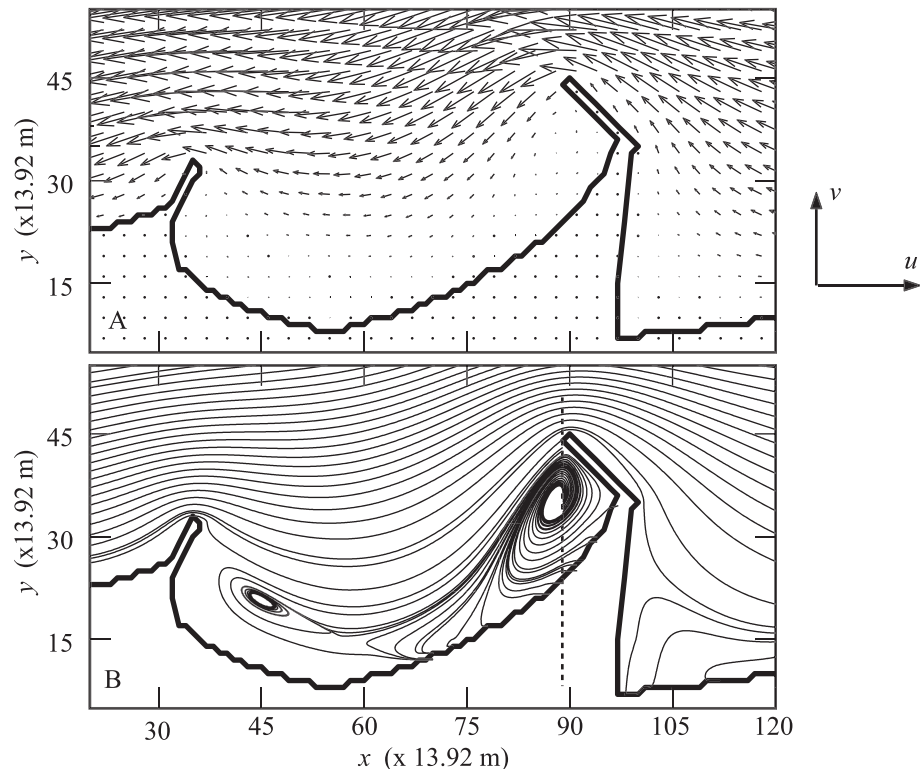


Fig. 13. Current pattern around the study beach with a shortened south breakwater driven by an upcoast longshore current with the same boundary conditions as described in Fig. 4. (A) Current velocity vectors; (B) streamlines. For clarity, streamlines inside the embayment start at selected points along the dotted vertical line.

to the bottom sediment, while a small percentage could eventually be released out of the embayment.

Discussion

Cases II and III in the Results have clearly illustrated the effect of the embayment structure of 63rd Street Beach on the transport and fate of *E. coli* nearshore. Admittedly, the embayment design is effective in preventing beach erosion. Nevertheless, an embayment with long breakwaters or jetties that significantly obstructs longshore currents also has the shortcoming of retaining excessive contaminants. The effectiveness of preventing beach erosion (i.e., retaining sediments) appears to be consistent with that of retaining contaminants because sands and contaminants are all passive scalars in nature and are transported similarly by a coastal flow field. Design of recreational beaches, although quite a new practice in coastal engineering, should consider balancing the needs of retaining sand and of maintaining water quality. One measure for remediation to consider might be the reduction of the lengths of the breakwaters and hence reducing the surface area of the embayment. The short breakwaters at 31st Street Beach (only one-half to one-third the lengths of those of 63rd Street Beach), for example, might have increased the flushing capacity of the embayment and hence yielded a significantly lower *E. coli* concentration (geometric mean 62 MPN 100 mL⁻¹;

Whitman and Nevers 2008). Although the optimal lengths and orientation of the breakwaters are anticipated to be beach specific, a computer-aided design approach using numerical models that combine physical and biological mechanisms, like the approach used in the present study, could be helpful. The design, however, can also be complicated by ecological (e.g., potential effects on the population of other species) and economical (e.g., cost) considerations.

As a preliminary attempt toward improving microbial water quality by modifying the design of the beach, we considered a hypothetical case in which we shortened the south breakwater to half its actual length. Holding all other settings the same as in case II, a numerical simulation, case III, predicted an overall improvement of *E. coli* contamination by nearly 20% and a reduction of potential source of *E. coli* by 11% (Table 2). In fact, these improvements can be explained by the nondimensional form of the model (Eq. 5). On the right side of Eq. 5, the nondimensional numbers D_a and \tilde{D}_a both explicitly have the length of the south breakwater B as a factor. Therefore, reducing B would decrease the contributions of these two bacterial decay terms by the same proportion and, hence, relatively augment the contribution of advective (i.e., flushing of the embayment). The embayment settling number E_m , however, is determined by the beach sloping characteristic β rather than by B individually. The scale of the contribution from settling would not be changed

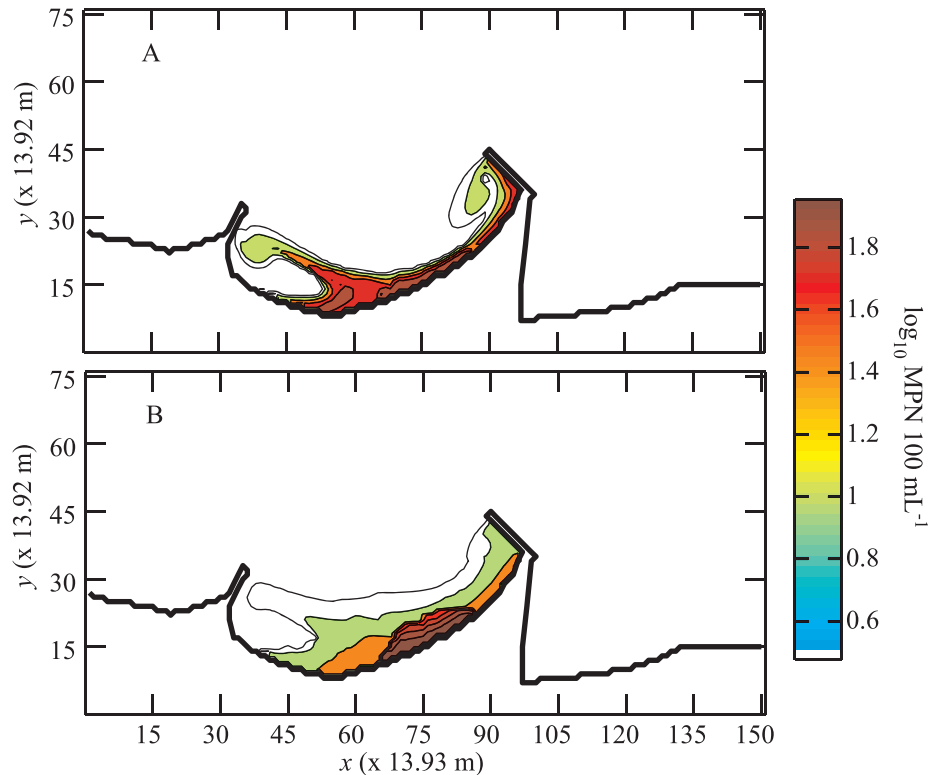


Fig. 14. Distributions of *E. coli* concentration at the eighth hour after a resuspension event in the embayment with a shortened south breakwater (case III) and an initial *E. coli* concentration the same as that of case II (Fig. 11). (A) Suspended culturable *E. coli* concentration; (B) settled culturable *E. coli* concentration.

significantly in response to the reduction in B . The settling of culturable *E. coli* inside the embayment would remain similar to that of case II, which is clearly demonstrated in Figs. 11B and 14B, and therefore its mitigation, if any, would be only marginal. Consequently, the resultant effect of shortening the south breakwater by 50% would lead to an improvement of *E. coli* contamination only by a lower rate (i.e., 10–20%). The outcome given in Table 2 is also due to the fact that the hydrodynamic system in the embayment was nonlinear (Figs. 4, 13) and the characteristic velocity U appeared insensitive to the change in B .

Abdelrhman (2005) noted that the flushing time T_f (h) of a dye that was assumed to be conservative and initially uniformly distributed in each of the 42 embayments was best

described by the (longshore) length, B' (km), and the surface area, A (km²), of the embayments. More specifically,

$$T_f = 22.05B' + 2.57A - 1.11B'^2 \quad (10)$$

($R^2 = 0.85$). The use of B' as the characteristic length of the embayment in Abdelrhman (2005) is not inconsistent with our use of the breakwater length because for most embayments these two lengths are of the same order of scale. The empirical relation (Eq. 10) should be considered as a common flushing characteristic of embayments where material settling, reaction, and the effect of water depth are all ignored. For his study, therefore, each embayment was essentially two-dimensional and dominated by advection, which can be described by Eq. 5 without right-side terms and hence is not comparable to the present study.

Table 2. Possible reduction of *E. coli* contamination by shortening the south breakwater.

Case	Breakwater length (m)	Embayment surface area (10 ⁵ m ²)	<i>E. coli</i> number (culturable) in the embayment (10 ¹⁰ MPN)			
			Suspended (10th hour)	Settled (10th hour)	Suspended (20th hour)	Settled (20th hour)
Original*	344	3.317	3.628	5.080	1.423	6.209
Shortened†	172	2.798	3.052	4.577	1.156	5.529
Reduction‡	50%	16%	16%	10%	19%	11%

* Case II in the present work.

† Case III in the present work.

‡ Reduction relative to the original case.

Table 3. Simulation results at the 20th hour with the same setting as case II but with different settling velocity values (w_s).

Settling velocity	$0.82 \cdot 10^{-5} \text{ m s}^{-1}$		$1.65 \cdot 10^{-5} \text{ m s}^{-1}$ (case II)		$3.3 \cdot 10^{-5} \text{ m s}^{-1}$	
	Suspended	Settled	Suspended	Settled	Suspended	Settled
Culturable <i>E. coli</i> number (10^{10} MPN)	2.757	3.519	1.423	6.209	0.731	7.971
Proportion	16.6%	21.2%	8.6%	37.3%	4.5%	47.9%

Since in the present work embayment flushing was considerably complicated by bacteria settling and decay as well as with a much finer spatial resolution, Eq. 10 should be significantly modified. Despite the differences, results from our hypothetical case III agreed qualitatively with those of Abdelrhman (2005) that reducing surface area (by shortening the south breakwater) could result in improved microbial water quality (reduced flushing time) to a certain degree, but a general form replacing Eq. 10 is beyond the scope of our work.

Cases I and II indicated the same major characteristic of the embayment: mass exchange between the inside and the outside was weak. This was due mainly to the existence of the breakwaters that absorbed a large amount of momentum and kinetic energy of the oncoming longshore currents, so that the circulation inside the embayment was driven mostly by lateral turbulent shearing. But there are also differences between these two cases, that is, the characteristic current velocity and the water depth. When the *E. coli* source was from the outside of the embayment where advection was dominant due to the greater water depth and current velocity, settling was not pronounced until part of the plume entered the embayment (refer to the discussion following Eq. 5). The embayed beach water had significantly different hydrodynamic characteristics from the outside, with the contributions of *E. coli* settling and decay comparable to that of advection. Conversely, when the *E. coli* source originated in the shallow water inside the embayment, settling might result in quick deposition. In this sense, embayment is a better receiver than releaser of *E. coli* under typical current conditions. As *E. coli* can often survive in the submerged sediment for an extended period of time (e.g., several months), the embayment serves as an *E. coli* sink, making recurrent resuspension–deposition cycles possible. When flushing is weak (case II), bacterial decay becomes the most effective mechanism for the reduction of culturable *E. coli* number in the embayment. Cloudiness or precipitation would further reduce the bacterial die-off, for the effect of solar inactivation of *E. coli* is then minimal.

Extending our ideal cases, we might have sufficient information to explain why 63rd Street Beach had distinctly high summer *E. coli* concentrations. Case I represents an episode of *E. coli* importation into the embayment. Although a single episode similar to case I cannot significantly affect the water quality at the beach, the embayment conceivably receives a number of similar *E. coli* loadings over a longer period of time (e.g., in a month). It is possible that *E. coli* settle and accumulate in the bottom sediment over a few loading episodes. When intense resuspension events take place, *E. coli* are reintroduced into the nearshore water

column and cause elevated *E. coli* densities. Case II represents more of a redistribution event than a releasing process of *E. coli* in the embayment. The total number of *E. coli* in the embayment thus reduces slowly over time. As intense wave actions that would cause resuspension frequently coincide with a storm event, the effect of solar inactivation can be much weaker than that in case II.

Wave action has been recognized as a major mechanism for *E. coli* loading from the submerged sediment (Fig. 8). When high waves propagate onshore toward the beach, the run-up on the beach face is also increased (Ge et al. 2010). This enhanced interaction of waves with the beach surface in the swash zone will possibly yield an additional loading of *E. coli* from the foreshore sand, which is often a storage of *E. coli* derived from multiple sources (e.g., birds and *Cladophora*; Whitman and Nevers 2003; Whitman et al. 2003; Ishii et al. 2007). This has been inferred from previous statistical analyses (Ge et al. 2010). Case II, therefore, can be viewed as the consequence of sediment resuspension in conjunction with beach washing due to severe wave actions. As gulls are frequently observed to gather or feed at the beachfront and in the nearshore water, direct *E. coli* input into the shallow water by bird droppings can be another source of contamination. This foreshore loading may not need wave actions but, according to case II, is equally difficult to release out of the embayment under typical current conditions.

Many more complicated scenarios can be deduced from the simple, fundamental cases studied here. For example, if the current flow outside the embayment reverses gradually during the period of case II, it is conceivable that the entire current field, both inside and outside the embayment, will slow down first prior to a reversal. This would further weaken the flushing of *E. coli* and equivalently increase sediment (*E. coli*) settling (Eq. 5). A real-time forecasting of coastal water quality, which is driven by time-varying hydrodynamic conditions in the embayment, is planned for future work.

Acknowledgments

We are grateful to David Schwab and Nathan Hawley of National Oceanic and Atmospheric Administration (NOAA) for their contributions to this research. We also thank Gregory Lang of NOAA and Pramod Thupaki, Jie Niu, and George Wimbrow of Michigan State University for their assistance with data and fieldwork, as well as the two anonymous reviewers and the associate editor for their insightful comments. This work was funded by the U.S. Geological Survey (USGS) Great Lakes Ocean Research Priorities Plan (ORPP), Great Lakes Restoration Initiative, and NOAA's Ocean and Human Health Initiative. This article is contribution 1664 of the USGS Great Lakes Science Center.

References

- ABDELRHMAN, M. A. 2005. Simplified modeling of flushing and residence times in 42 embayments in New England, USA, with special attention to Greenwich Bay, Rhode Island. *Estuar. Coast. Shelf Sci.* **62**: 339–351, doi:10.1016/j.ecss.2004.09.021
- AMERICAN PUBLIC HEALTH ASSOCIATION. 1998. Standard methods for the examination of water and wastewater, 20th ed. American Public Health Association.
- AUER, M. T., AND S. L. NIEHAUS. 1993. Modeling fecal coliform bacteria—I. Field and laboratory determination of loss kinetics. *Water Res.* **27**: 693–701, doi:10.1016/0043-1354(93)90179-L
- BAI, S., AND W.-S. LUNG. 2005. Modeling sediment impact on the transport of fecal bacteria. *Water Res.* **39**: 5232–5240, doi:10.1016/j.watres.2005.10.013
- BELETSKY, D., AND D. J. SCHWAB. 2001. Modeling circulation and thermal structure in Lake Michigan: Annual cycle and interannual variability. *J. Geophys. Res.* **106**: 19745–19771, doi:10.1029/2000JC000691
- BERKHOFF, J. C. W., N. BOOY, AND A. C. RADDER. 1982. Verification of numerical wave propagation models for simple harmonic linear water waves. *Coast. Eng.* **6**: 255–279, doi:10.1016/0378-3839(82)90022-9
- BURTON, G. A., JR., D. GUNNISON, AND G. R. LANZA. 1987. Survival of pathogenic bacteria in various freshwater sediments. *Appl. Environ. Microbiol.* **53**: 633–638.
- CHAPRA, S. C. 1997. Surface water-quality modeling. McGraw-Hill.
- CHO, K. H., Y. A. PACHEPSKY, J. H. KIM, A. K. GUBER, D. R. SHELTON, AND R. ROWLAND. 2010. Release of *Escherichia coli* from the bottom sediment in a first-order creek: Experiment and reach-specific modeling. *J. Hydrol.* **391**: 322–332, doi:10.1016/j.jhydrol.2010.07.033
- DAVIES, C. M., J. A. H. LONG, M. DONALD, AND N. J. ASHBOLT. 1995. Survival of fecal microorganisms in marine and freshwater sediments. *Appl. Environ. Microbiol.* **61**: 1888–1896.
- DE BRAUWERE, A., B. DE BRYE, P. SERVAIS, J. PASSERAT, AND E. DELEERSNIJDER. 2011. Modelling *Escherichia coli* concentrations in the tidal Scheldt river and estuary. *Water Res.* **45**: 2724–2738, doi:10.1016/j.watres.2011.02.003
- DEAN, R. G., AND R. A. DALRYMPLE. 1984. Water wave mechanics for engineers and scientists. Prentice Hall.
- ECKNER, K. F. 1998. Comparison of membrane filtration and multiple-tube fermentation by the Colilert and Enterolert methods for detection of waterborne coliform bacteria, *Escherichia coli*, and enterococci used in drinking water and bathing water quality monitoring in southern Sweden. *Appl. Environ. Microbiol.* **64**: 3079–3083.
- FRICK, W. E., Z. GE, AND R. G. ZEPP. 2008. Nowcasting and forecasting concentrations of biological contaminants at beaches: A feasibility and case study. *Environ. Sci. Technol.* **42**: 4818–4824, doi:10.1021/es703185p
- GE, Z., M. B. NEVERS, D. J. SCHWAB, AND R. L. WHITMAN. 2010. Coastal loading and transport of *Escherichia coli* at an embayed beach in Lake Michigan. *Environ. Sci. Technol.* **44**: 6731–6737, doi:10.1021/es100797r
- GOYAL, S. M., C. P. GERBA, AND J. L. MELNICK. 1977. Occurrence and distribution of bacterial indicators and pathogens in canal communities along the Texas coast. *Appl. Environ. Microbiol.* **34**: 139–149.
- GRANT, S. B., AND B. F. SANDERS. 2010. Beach boundary layer: A framework for addressing recreational water quality impairment at enclosed beaches. *Environ. Sci. Technol.* **44**: 8804–8813, doi:10.1021/es101732m
- GRANT, W. D., AND O. S. MADSEN. 1986. The continental-shelf bottom boundary layer. *Annu. Rev. Fluid Mech.* **18**: 265–305, doi:10.1146/annurev.fl.18.010186.001405
- HALLER, L., J. POTE, J. L. LOIZEAU, AND W. WILDI. 2009. Distribution and survival of faecal indicator bacteria in the sediments of the Bay of Vidy, Lake Geneva, Switzerland. *Ecol. Indic.* **9**: 540–547, doi:10.1016/j.ecolind.2008.08.001
- HAWLEY, N., AND C. LEE. 1999. Sediment resuspension and transport in Lake Michigan during the unstratified period. *Sedimentology* **46**: 791–805, doi:10.1046/j.1365-3091.1999.00251.x
- HIPSEY, M. R., J. P. ANTENUCCI, AND J. D. BROOKES. 2008. A generic, process-based model of microbial pollution in aquatic systems. *Water Resour. Res.* **44**: W07408, doi:10.1029/2007WR006395
- , J. D. BROOKES, R. H. REGEL, J. P. ANTENUCCI, AND M. D. BURCH. 2006. In situ evidence for the association of total coliforms and *Escherichia coli* with suspended inorganic particles in an Australian reservoir. *Water Air Soil Pollut.* **170**: 191–209, doi:10.1007/s11270-006-3010-6
- HU, J. Y., X. N. CHU, P. H. QUEK, Y. Y. FENG, AND X. L. TAN. 2005. Repair and regrowth of *Escherichia coli* after low- and medium-pressure ultraviolet disinfection. *Water Supply* **5**: 101–108.
- ISHII, S., D. L. HANSEN, R. E. HICKS, AND M. J. SADOWSKY. 2007. Beach sand and sediments are temporal sinks and sources of *Escherichia coli* in Lake Superior. *Environ. Sci. Technol.* **41**: 2203–2209, doi:10.1021/es0623156
- LEE, C., D. J. SCHWAB, D. BELETSKY, J. STROUD, AND B. M. LESHT. 2007. Numerical modeling of mixed sediment resuspension, transport, and deposition during the March 1998 episodic events in southern Lake Michigan. *J. Geophys. Res.* **112**: C02018, doi:10.1029/2005JC003419
- LIU, L., M. S. PHANIKUMAR, S. L. MOLLOY, R. L. WHITMAN, D. A. SHIVELY, M. B. NEVERS, D. J. SCHWAB, AND J. B. ROSE. 2006. Modeling the transport and inactivation of *E. coli* and enterococci in the near-shore region of Lake Michigan. *Environ. Sci. Technol.* **40**: 5022–5028, doi:10.1021/es060438k
- LOU, J., AND S. R. MASSEL. 1994. A combined refraction-diffraction-dissipation model of wave propagation. *Chin. J. Oceanol. Limnol.* **12**: 361–371, doi:10.1007/BF02850497
- , P. V. RIDD, C. L. MAYOCCHI, AND M. L. HERON. 1996. Wave-induced benthic velocity variations in shallow waters. *Estuar. Coast. Shelf Sci.* **42**: 787–802, doi:10.1006/ecss.1996.0050
- , D. J. SCHWAB, D. BELETSKY, AND N. HAWLEY. 2000. A model of sediment resuspension and transport dynamics in southern Lake Michigan. *J. Geophys. Res.* **105**: 6591–6610, doi:10.1029/1999JC900325
- MAHLER, B. J., J.-C. PERSONNE, G. F. LODS, AND C. DROGUE. 2000. Transport of free and particulate-associated bacteria in karst. *J. Hydrol.* **238**: 179–193, doi:10.1016/S0022-1694(00)00324-3
- MELLOR, G. L. 2004. Users guide for a three-dimensional, primitive equation, numerical ocean model. Princeton University, http://jes.apl.washington.edu/modsims_two/usersguide0604.pdf
- NEVERS, M. B., AND R. L. WHITMAN. 2005. Nowcast modeling of *Escherichia coli* concentrations at multiple urban beaches of southern Lake Michigan. *Water Res.* **39**: 5250–5260, doi:10.1016/j.watres.2005.10.012
- NIELSEN, P. 1992. Coastal bottom boundary layers and sediment transport. World Scientific.
- OLYPHANT, G. A., AND R. L. WHITMAN. 2004. Elements of a predictive model for determining beach closures on a real time basis: The case of 63rd Street Beach Chicago. *Environ. Monit. Assess.* **98**: 175–190, doi:10.1023/B:EMAS.0000038185.79137.b9
- QUEK, P. H., AND J. HU. 2008. Influence of photoreactivating light intensity and incubation temperature on photoreactivation of *Escherichia coli* following LP and MP UV disinfection. *J. Appl. Microbiol.* **105**: 124–133, doi:10.1111/j.1365-2672.2008.03723.x

- REHMANN, C. R., AND M. L. SOUPIR. 2009. Importance of interactions between the water column and the sediment for microbial concentrations in streams. *Water Res.* **43**: 4579–4589, doi:10.1016/j.watres.2009.06.049
- STEETS, B. M., AND P. A. HOLDEN. 2003. A mechanistic model of runoff-associated fecal coliform fate and transport through a coastal lagoon. *Water Res.* **37**: 589–608, doi:10.1016/S0043-1354(02)00312-3
- THUPAKI, P., M. S. PHANIKUMAR, D. BELETSKY, D. J. SCHWAB, M. B. NEVERS, AND R. L. WHITMAN. 2010. Budget analysis of *Escherichia coli* at a southern Lake Michigan beach. *Environ. Sci. Technol.* **44**: 1010–1016, doi:10.1021/es902232a
- WHITMAN, R. L., AND M. B. NEVERS. 2003. Foreshore sand as a source of *Escherichia coli* in nearshore water of a Lake Michigan beach. *Appl. Environ. Microbiol.* **69**: 5555–5562, doi:10.1128/AEM.69.9.5555-5562.2003
- , AND ———. 2008. Summer *E. coli* patterns and responses along 23 Chicago beaches. *Environ. Sci. Technol.* **42**: 9217–9224, doi:10.1021/es8019758
- , ———, G. C. KORINEK, AND M. N. BYAPPANAHALLI. 2004. Solar and temporal effects on *Escherichia coli* concentration at a Lake Michigan swimming beach. *Appl. Environ. Microbiol.* **70**: 4276–4285, doi:10.1128/AEM.70.7.4276-4285.2004
- , D. A. SHIVELY, H. PAWLIK, M. B. NEVERS, AND M. N. BYAPPANAHALLI. 2003. Occurrence of *Escherichia coli* and enterococci in *Cladophora* (Chlorophyta) in nearshore water and beach sand of Lake Michigan. *Appl. Environ. Microbiol.* **69**: 4714–4719, doi:10.1128/AEM.69.8.4714-4719.2003
- ZHU, X., J. D. WANG, H. M. SOLO-GABRIELE, AND L. E. FLEMING. 2011. A water quality modeling study of non-point sources at recreational marine beaches. *Water Res.* **45**: 2985–2995, doi:10.1016/j.watres.2011.03.015

Associate editor: Chris Rehmann

Received: 29 October 2010
Accepted: 30 September 2011
Amended: 23 October 2011